

## SPIN-ORBIT COUPLING INDUCED CHEMICAL REACTIVITY AND SPIN-CATALYSIS PHENOMENA

Boris F. MINAEV and Hans AGREN

*Institute of Physics and Measurement Technology,  
University of Linköping, S-58183, Linköping, Sweden*

Received July 13, 1994  
Accepted December 5, 1994

1. Introduction .....	340
2. Chemical Reactions Governed by Spin-Orbit Coupling .....	342
2.1. Spin-Orbit Coupling Effects in Chemically Induced Dynamic Nuclear Polarization (CIDNP). Photolysis of Cyclohexanone .....	342
2.2. Other Photochemical Reactions of Carbonyl Compounds .....	345
2.3. Photoisomerization and Fragmentation of Furans .....	348
2.4. Spin-Orbit Coupling Effects in Reactions of Atomic Oxygen O( <sup>3</sup> P) with Hydrocarbons ..	348
2.5. Spin-Orbit Coupling Effects in Reactions of Molecular Oxygen with Unsaturated Hydrocarbons .....	352
3. The Mechanism of the External Heavy Atom Spin-Catalysis .....	354
4. Spin-Catalysis by Transition Metal Compounds .....	357
4.1. Intersystem Crossing Localized at the Transition Metal Site .....	359
4.2. Spin-Photocatalysis .....	361
5. Paramagnetic Exchange Spin-Catalysis .....	364
6. Oxygen Activation by Metal Complexes and Oxidation Spin-Catalysts .....	366
7. Summary .....	367
Acronyms .....	368
References .....	369

The crucial role of electron spin in the control of the reaction channels in the region of activated complexes can easily be inferred from the general principles of chemical bonding. Magnetic perturbations could change spin at the intermediate stages of a reaction or in the region of activation barriers and could hence influence the reaction rate through spin switching of the reaction paths. Spin-orbit coupling is one of the most important intrinsic magnetic perturbations in molecules; its role in chemical reactivity is here shown by a few typical examples. Spin-orbit coupling induced spin flip could also be important in catalysis by transition metals. General qualitative arguments predict great enhancements of the spin-orbit coupling in catalytic complexes with transition metal compounds. The concept of spin-catalysis is introduced in order to describe and classify a wide range of phenomena in which chemical reactions are promoted by substances assisting in inducing spin changes and overcoming spin-prohibition. This concept is based on results of quantum chemical calculations with account of spin-orbit coupling and configuration interaction in the intermediate complexes. Besides spin-orbit coupling, the role of intermolecular exchange interaction with open shell catalysts is stressed. The catalytic action would definitely depend on the efficiency of spin uncoupling inside the reacting substrate molecule and this could be induced by magnetic and exchange perturbations.

## 1. INTRODUCTION

From the generalization of valence bond theory it follows that the chemical bond is formed because of overlap of two atomic orbitals which contain two electrons with opposite spins<sup>1</sup>. Because of this, the majority of stable substances in organic chemistry are diamagnetic. They have a singlet (S) ground state well separated in energy from the excited triplet (T) state. However, in the course of a chemical rearrangement at the vicinity of an activated barrier where chemical bonds grow weak, the singlet-triplet (S-T) energy gap decreases drastically and an S-T crossing could be possible. This is obvious for reactions proceeding through a diradical stage. The possibility of S-T transitions must be taken into account for a large number of chemical reactions<sup>2,3</sup>. A few examples are considered in this article. If the orbital structure of S and T states does not allow them to get mixed by spin-orbit coupling (SOC) in the intermediate stage of a reaction (as it is in the case of oxidation by air oxygen<sup>4</sup>), spin-catalysis could be important. The choice of catalyst, which assists and accelerates the S-T intersystem crossing, could be used as a controlling factor of chemical processes<sup>5</sup>. In general, not only S-T transitions should be considered, but any changes of spin multiplicity involved in chemical rearrangements. The most important perturbations responsible for the total spin change in catalysant species during the catalyst-substrate interaction are spin-orbit coupling (SOC) and intermolecular exchange interaction with a paramagnetic catalyst. The transition metal complexes, being the most popular homogeneous catalysts, constitute also a very important subject for spin-catalysis. They have typically few near-degenerate excited states just above the ground state with different orbital and spin symmetry because of small crystal field splittings of *d* shells. This is often the reason that SOC effects manifest themselves in UV and ESR spectra of such systems, providing large orbital magnetism. Supplying its *d* orbitals for the common states of the catalytic system (through different charge transfer and local state admixtures in a configuration interaction description) a transition metal atom can promote a large shift of orbital angular momentum during the S-T transition inside the reacting system, thereby enhancing SOC and effectively removing the spin-prohibition. Spin-catalysis seems to be a common feature for many biological processes. The spin-change transformations occurring in iron complexes in particular are related to oxygenation and carbonylation of hemoglobin<sup>6</sup>. The transition metal sites in metalloenzymes catalyze the reactions of paramagnetic molecular oxygen with diamagnetic organic substrates.

The second type of spin-catalysts are paramagnetic substances, which supply their unpaired electrons during the catalytic contact with diamagnetic molecules in order to assist the S-T transition in its chemical rearrangement. The nature of this catalysis is not connected with magnetic perturbation, which is negligible, but is determined by intermolecular exchange and charge transfer interaction<sup>4</sup>. The relevant examples are catalysis of decarboxylation of malonic acids by paramagnetic rare earth ions<sup>7</sup> and the gas phase thermal *cis-trans* isomerization and polymerization reactions of olefines cata-

lyzed by NO, O<sub>2</sub> and by other paramagnetic species<sup>8</sup>. Catalytic isomerization of quadricyclane to norbornadiene<sup>9</sup> seems to be of paramagnetic spin-catalytic nature. Some enzyme catalyzed oxidation reactions provide other examples of this category<sup>10</sup>. The nature of spin uncoupling produced by paramagnetic catalysts is yet not well understood. In some examples we can see connections between this type of spin-catalysis and one-electron oxidation of organic substrates<sup>4,11</sup>. We can also refer to the theory<sup>9</sup> treating the exchange interaction between different combinations of spin multiplets of open shell transition metal catalysts and organic reagents. The authors of ref. 9 have used an effective Hamiltonian method for reactant-catalyst open-shell systems and stressed the importance of configuration interaction in contrast to the simple orbital correlation diagrams of the Mango-Schachtschneider theory<sup>12</sup>. They obtained S and T potential energy surfaces that touch each other at the transition state region in organic substrate reactions, and that begin to repel each other under the influence of the paramagnetic metal complex. The resulting reduction of activation energy by such spin uncoupling is an indication of paramagnetic exchange spin-catalysis.

The other types of spin-catalysis could be briefly classified as follows. Photosensitized reactions include the combination of a SOC effect inside the catalyst (sensitizer) and an intermolecular exchange interaction governing the T-T energy transfer to the catalysant. There can be also other types of energy transfers, including simultaneous multiplicity changes in both species, catalyst and catalysant. The generation of singlet oxygen O<sub>2</sub>(<sup>1</sup>Δ<sub>g</sub>) by light absorption of rose bengale, adsorbed on zeolite with subsequent oxidation of the organic substrate is one out of a great variety of examples of this type of spin-catalysis.

The next, fourth type of chemical reactions with spin-promoted acceleration is connected with electrochemical or thermal generation of spin-active particles (radicals, diradicals, ionradical pairs, etc.). The examples of the fourth type of processes are so numerous that it is difficult to survey them in a short sketch. The scope for this mechanism of spin uncoupling comprises many types of redox catalysis<sup>4,5</sup>. The assignment of them to spin-catalysis could be somewhat questionable, but electrochemical generation of singlet oxygen<sup>13</sup> and of organic radicals in electrochemical modification of alkaloids<sup>14</sup> gives definite confidence to that other relevant processes should be considered as spin-catalysis phenomena of similar types. We mean that electrochemical cycles with electron transfer through interfaces can include both types of spin uncoupling; SOC induced reactions and paramagnetic-exchange enhanced processes.

The fifth type of spin-catalysis, namely chemical reactions governed by an external magnetic field, could have different mechanisms. The two most important of these, described by the radical pair theory and by triplet mechanisms, are well studied and have numerous applications in many areas of chemistry and biochemistry<sup>15-17</sup>. The studies of chemically induced dynamic nuclear polarization (CIDNP) have directed the attention to the role of S-T transitions in radical recombination reactions and to the

magnetic field effects in chemical reactivity<sup>16</sup>. Because the external magnetic field (MF) influence on spin uncoupling in reacting molecules is similar in some way to SOC induced perturbations, we can consider the MF effects as spin-catalysis of physical nature. The examples of the main two types of spin-catalysis are considered in the following by calculations of simple models. Short generalizations are derived for different classes of catalysts and reaction conditions. Firstly we consider reactions which are simultaneously forbidden by orbital and by spin symmetry selection rules and we formulate conditions when such reactions become effectively allowed by SOC.

## 2. CHEMICAL REACTIONS GOVERNED BY SPIN-ORBIT COUPLING

In this section we present few examples of chemical reactions proceeding through the singlet-triplet transitions. These reactions are effectively allowed by large spin-orbit coupling; a prerequisite for this is given by one-center orbital rotations during the S-T transition which induce a torque for the spin flip<sup>2,3</sup>. High topicity of the reactions is necessary as well as double forbidness by orbital and by spin symmetry selection rules<sup>3</sup>. The concept of "topicity" was introduced by Salem<sup>1,25</sup> in order to determine the total number of available radical sites generated in the primary process and also to specify the symmetry of each site. This concept is quite important for the analysis and classification of SOC effects in chemical reactions<sup>3</sup>.

### 2.1. Spin-Orbit Coupling Effects in Chemically Induced Dynamic Nuclear Polarization (CIDNP). Photolysis of Cyclohexanone

CIDNP is manifested in abnormal enhancements of NMR absorption intensities or even in NMR emission<sup>16</sup>. The nonequilibrium populations of nuclear spin sublevels pumped during a chemical reaction, CIDNP, is very sensitive to weak magnetic perturbations on the intermediate stages of the chemical process. Normally it is treated in the framework of the Radical Pair Theory (RPT)<sup>16</sup>, where the singlet-triplet ( $S-T_0$ ) state mixing in the separated RP is induced by extremely weak hyperfine coupling of electron and nuclear spins, provided the time spent in the mixing region is sufficiently long. The same type of theory has been applied to CIDNP and magnetic field effects in reactions proceeding through diradical intermediates<sup>18</sup>. Two radical sites separated by long flexible  $-(CH_2)_n-$  chains in diradicals can recombine in the same manner like geminate radical pairs in solution. But for the short-chain diradicals ( $n \leq 8$ ) and for the diradicals of acyl-alkyl type, interactions independent of the nuclear spin must be involved in order to explain the S-T mixing and observed CIDNP (ref.<sup>18</sup>). Cycloalkanone photolysis shows absorption spectra which seem to follow the  $T_0-S$  polarization. Investigations of the field dependence of CIDNP for  $^1H$  and  $^{13}C$  have shown contrasting behaviour for strong magnetic fields. In the attempts to explain the cyclohexanone results it was suggested<sup>18</sup> that spin-orbit coupling accompanied by product selectivity provides an alter-

native pathway for intersystem crossing (ISC) in the diradicals. A qualitative explanation of the reversible  $\alpha$ -cleavage reaction of cyclohexanone can be obtained from the simple resonance structures of some active valence electrons for ground and lowest excited states of both the reactant and the primary products, neglecting the out-of-plane deformation. These structures were calculated by the MNDO CI method and are shown qualitatively in the Fig. 1. The symmetry and number of active electrons for the planar structures are also indicated. After the  $S_0 \rightarrow T(n\pi^*)$  excitation of cyclohexanone the triplet  ${}^3D_{\sigma\pi}$  diradical can easily be formed (Fig. 1). Because of vibrations in the diradical the  $S_0-T_1$  crossing is reached frequently. In that case the T-S transition rate is directly determined by the square of the SOC matrix element. Let us consider the qualitative features of the spin-orbit coupling.

In the  $S_0({}^1D_{\sigma\sigma})-T_1({}^3D_{\sigma\pi})$  crossing both structures differ by rotation of the  $2p$  AO on the oxygen atom. Such a rotation produces a flash of orbital angular momentum during

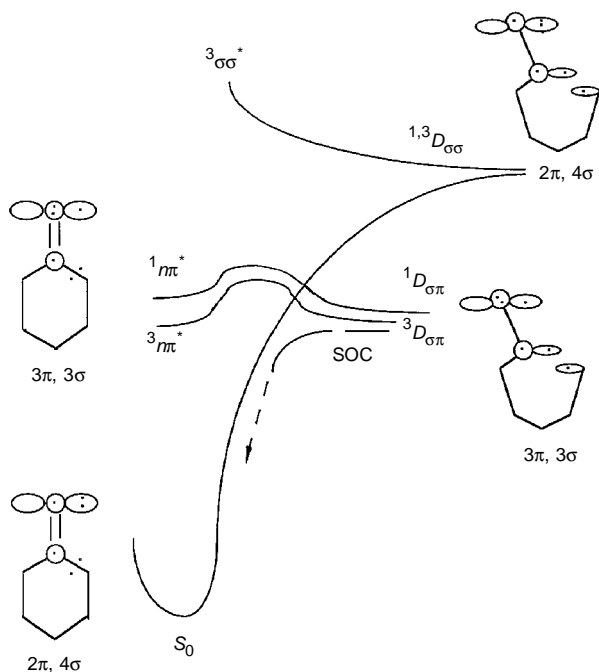


FIG. 1

Cross sections of qualitative potential energy surface along the reaction path of the photochemical reversible  $\alpha$ -cleavage of cyclohexanone

the T–S transition which “interacts” with spin change ( $\Delta S = 1$ ). In this case the SOC matrix element between the  $S_0$  and  $T_1$  states should be very large, like in the pure oxygen atom. Rotation of the  $2p$  electrons in the  $O(^3P)$  atom corresponds (in a “quantum sense”) to conservation of the orbital angular momentum ( $L = 1$ ) as an observable; finally this leads to the SOC between  $\mathbf{L}$  and  $\mathbf{S}$  angular moments and to the SOC splitting for different  $J$  values. This splitting is comparatively large in the  $O(^3P)$  atom;  $E(J = 2) - E(J = 1) = \zeta_O = 153 \text{ cm}^{-1}$ , which is much larger, for example, than the SOC splitting in the carbon atom ( $\zeta_C = 29 \text{ cm}^{-1}$ ). The SOC matrix element between singlet ( $^1D$ ) and triplet ( $^3P_2$ ) states is of the order magnitude of  $\zeta$ . It is equal to  $2^{1/2}\zeta$  in a single configuration approach;  $\zeta$  is here a SOC constant and determines the largest possible SOC energy in the neutral atom. In general, SOC can be observed as a multiplet splitting in the systems which conserve the orbital angular momentum,  $\mathbf{L}$  (atoms, diatomic and other linear molecules). In polyatomic molecules with lower symmetry,  $\mathbf{L}$  is normally quenched, even so in states with orbital degeneracy because of Jahn–Teller effects (see, however, refs<sup>19,20</sup>). Therefore the triplet state splitting observed by ESR spectra in organic excited molecules and diradicals is normally very small (the zero field splitting, ZFS, is of the order of  $0.1 \text{ cm}^{-1}$ ) and the SOC contribution to the ZFS is often negligible<sup>20,21</sup>. But the fact that the orbital angular momentum in organic molecules is quenched does not mean that all other SOC effects should be quenched. This seems to be natural from the simple “classical” interpretation of SOC as a magnetic interaction between  $\mathbf{L}$  and  $\mathbf{S}$  moments. Quantum effects of S–T transitions induced by SOC are known in molecules as well as in atoms<sup>17,22</sup>. S–T matrix elements of the SOC operator

$$\langle S | \mathbf{H}_{\text{SO}} | T \rangle = \langle a_{\text{ST}} \rangle$$

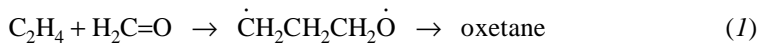
which mix singlet and triplet states and make transitions between them allowed, could be non-zero in molecules though  $\mathbf{L}$  is not conserved as a physical observable. Hence  $\langle a_{\text{ST}} \rangle$  would depend on the orbital angular momentum shift, which is induced “during” the S–T transition. Strictly speaking, this quantum integral has no direct physical interpretation; it has an imaginary value and only the absolute, squared, integral  $|\langle a_{\text{ST}} \rangle|^2$  is applied for the S–T transition rate constant calculations. Nevertheless, it seems to be useful to consider the idea that the orbital angular momentum induced during the S–T transition produces the torque which is necessary for the spin flip. The way the  $\langle a_{\text{ST}} \rangle$  value evolves depends on orbital symmetry and structure of the S and T states. If both states differ by orbital rotation on some atoms the  $\langle a_{\text{ST}} \rangle$  value would be non-zero. The value depends strongly on the nuclear charge of the atoms involved into this rotation<sup>17, 22</sup>.

Now let us go back to the intersystem crossing in the cyclohexanone diradical. The T–S transition shown by a dashed line on Fig. 1 involves  $n-\pi^*$  revolving on oxygen, the heaviest atom of the diradical. The ISC from the diradical to the ground state cyclohex-

anone includes both the orbital symmetry and spin multiplicity changes. Such double prohibition by spin and orbital symmetry selection rules leads to effectively allowed chemical process – reversible cyclization to the initial singlet ground state molecule. The SOC matrix element obtained by MNDO CISD calculations in the region of S–T crossing ranges in the interval 12 – 16 cm<sup>-1</sup>. This is only a small part of the maximum possible SOC value ( $\langle a_{ST} \rangle = 2^{-1/2} \zeta = 105 \text{ cm}^{-1}$ ), because of delocalization of the  $n$  and  $\pi$  electrons. The  ${}^3D_{\sigma\pi}$  wave function in the region of S–T crossing includes only a part of a highly localized  $n\pi^*$  structure and the singlet state is a mixture of many configurations. Although the real picture does not completely coincide with the oversimplified resonance structures, shown in Fig. 1, the qualitatively large SOC can be explained<sup>2,23</sup>. Triplet  $D_{\sigma\pi}$  diradicals which escape the  $T \rightarrow S_0$  ISC and recyclization to the initial cyclohexanone are strongly spin-polarized because the SOC is highly anisotropic. Only the  $T^z$  ZFS spin sublevel leads to the product ( $z$  axis is along the C=O bond), other spin sublevels have much slower ISC rate constants to the  $S_0$  state. They can undergo ISC  $T \rightarrow S$  transitions inside the pure  $D_{\sigma\pi}$  diradical which are induced by the hyperfine coupling mechanism. The corresponding aldehyde products also exhibit strong CIDNP.

## 2.2. Other Photochemical Reactions of Carbonyl Compounds

The photochemical addition of carbonyl compounds to alkenes (the Paterno–Büchi reaction) has been extensively investigated<sup>24–27</sup>. As the simplest model of this reaction we can consider the addition of ethene to  ${}^3n\pi^*$  excited formaldehyde to form oxetane.



It is well established<sup>26,28</sup> that the Paterno–Büchi reactions proceed through the 1,4-diradical intermediate. We propose that diradical (I) is formed by a C–C attack, though it is not definitely known from experimental data if the 1,4-diradical formed by a C–O attack should be excluded. The latter diradical  $\dot{\text{C}}\text{H}_2\text{CH}_2\text{O}\dot{\text{C}}\text{H}_2$  is more often assumed in the literature<sup>24–26</sup> because it better corresponds to the hypothesis of a preliminary formation of the exciplex<sup>26</sup>  $\text{C}_2\text{H}_4^+ \cdot \text{CH}_2\text{O}^-$ . On the ground of *ab initio* calculations<sup>27</sup> it has been suggested that both diradical mechanisms may operate in the photochemical oxetane formation, though the diradical region corresponding to the C–C attack lies 10 kcal/mol lower in energy than the C–O region. Thus while the C–O attack is often used for mechanistic discussions<sup>24–26</sup>, the C–C mechanism of diradical formation still merits a serious consideration<sup>27</sup>. We can now show that only the C–C path of the first step approach can explain the high reactivity of the triplet excited  $n\pi^*$  state of carbonyl molecules in Paterno–Büchi photoreactions. Two possible diradical states are shown in Fig. 2a. The diradical formation reaction (I) is the  $\sigma(\sigma\pi)$  triplet process; one radical

$\sigma$ -site is on carbon atom and two possible ( $\sigma\pi$ )-radical sites are on oxygen atom (in respect to the CCCO plane, Fig. 2a). The  $^3D_{\pi\sigma}$  state is the initial state obtained by the C–C attack of the  $^3n\pi^*$  carbonyl to ethene. The  $n$  and  $\pi$  labels around the oxygen atom in Fig. 2a refer to atomic orbitals of the separated carbonyl molecule (their symmetry notations are opposite with respect to the diradical CCCO symmetry plane). The system

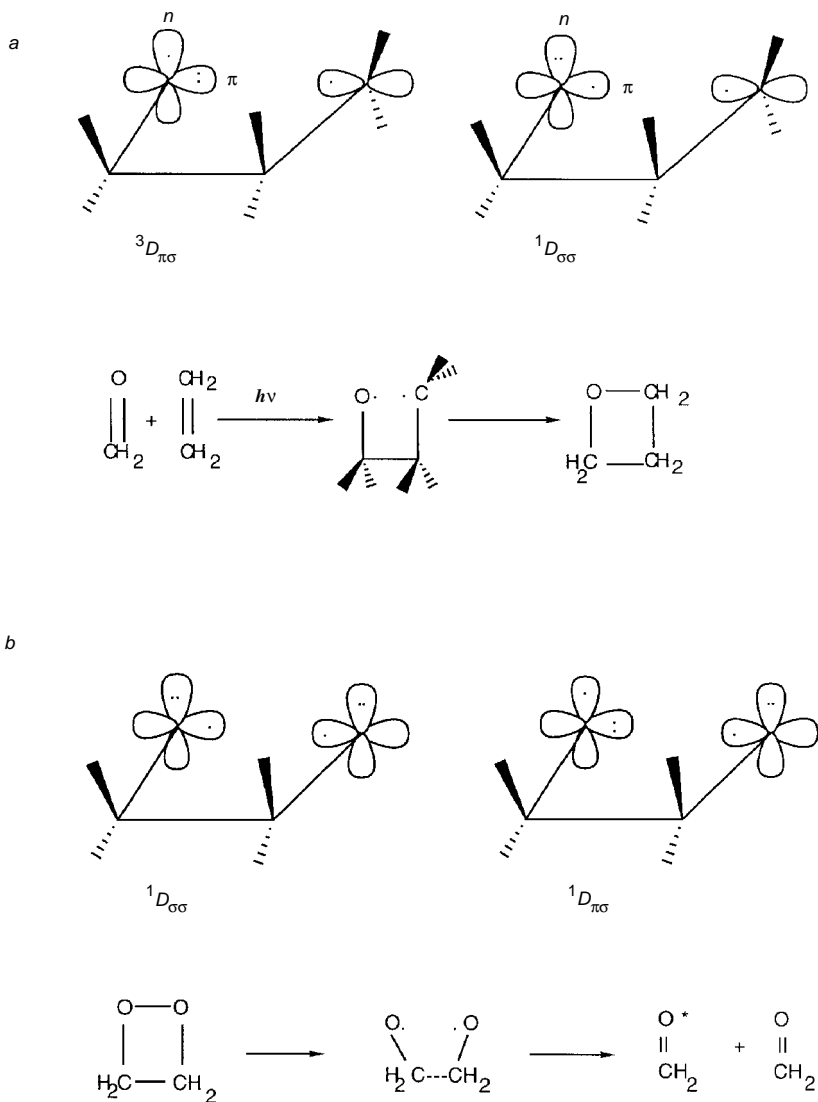


FIG. 2

Orbital structure of two possible states in diradicals produced by C–C attack in Paterno–Büchi reaction



must find an efficient ISC path since the initial triplet state of the reagents finally produces the singlet ground state oxetane. Such ISC is organized at the diradical stage as is illustrated by Fig. 2a. The triplet–singlet  ${}^3D_{\pi\sigma} \rightarrow {}^1D_{\sigma\sigma}$  transition is induced by large SOC because of the pure orbital rotation on the oxygen atom during the transition. After the ISC process the produced  ${}^1D_{\sigma\sigma}$  diradical develops immediately to the oxetane product, because all requirements for the C–O bond formation are fulfilled. The optimized triplet  ${}^3D_{\pi\sigma}$  diradical structure lies at the point of a conical intersection of the ground and excited singlet states<sup>27</sup>. Though the planar CCCO structures shown in Fig. 2a are oversimplifications of the real non-planar geometries<sup>27</sup>, this is not very important for the SOC analysis. The dihedral CCCO angle in triplet *gauche* diradical minima is  $62^\circ$  (which is close to MINDO/3 result<sup>29</sup>), but the SOC matrix element  $\langle a_{ST} \rangle$  does not deviate much from the maximum possible value,  $0.5 \zeta_0$ , between two diradicals shown<sup>29</sup> in Fig. 2a. This explains the relatively high quantum yield of oxetane production in the T state photosensitized Paterno–Buchi reaction. For the diradical obtained by the C–O attack the SOC matrix element should be an order of magnitude smaller<sup>29</sup> because it corresponds to two  $\dot{\text{C}}\text{H}_2\text{CH}_2\text{O}\dot{\text{C}}\text{H}_2$  structures with different rotations of the  $\text{CH}_2$  group on the ethene termini. None of them can induce large SOC for the T–S transition to the reactive singlet state in the conical intersection region. We can consider the C–O attack as an effectively spin-forbidden process in the T state photosensitized Paterno–Buchi reaction.

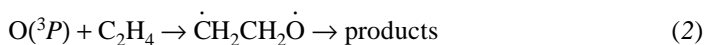
Quite similar SOC analysis was firstly performed by Turro and Devaquet for the chemiluminescent reaction of 1,2-dioxetane decomposition<sup>30</sup>. Thermal cleavage of the O–O bond during the dioxetane thermolysis produces a  $\dot{\text{O}}\text{CH}_2\text{CH}_2\dot{\text{O}}$  diradical in the  ${}^1D_{\sigma\sigma}$  state (Fig. 2b), which probably is quite close to the conical intersection with the excited singlet state. The triplet  $\pi$ ,  $\sigma^*$  excited dioxetane correlates with the  ${}^3D_{\pi\sigma}$  state of this diradical (Fig. 2b). The in-phase resonance of  $\sigma_a\pi_b$  and  $\pi_a\sigma_b$  configurations should in general be considered instead of the simple “nonresonant”  ${}^3D_{\pi\sigma}$  structure<sup>30</sup> (Fig. 2b). It does, however, not influence the qualitative analysis of SOC, because in the S–T intersection region the real diradical structure is not symmetric at all<sup>31</sup>. MINDO/3 calculations<sup>31</sup> predict the S–T crossing in the vicinity of the diradical when the O–O distance is quite large (1.84 Å) and the dihedral COOC angle is  $31.4^\circ$ . MINDO/3 CISD calculations<sup>29</sup> still predict a very large  $\langle a_{ST} \rangle$  SOC matrix element ( $39 \text{ cm}^{-1}$ ) at this geometry. This is in fact similar to the simple prediction ( $0.5 \zeta_0$ ), which follows from the oversimplified structures shown in Fig. 2b. After the  $S \rightarrow T$  transition the produced  ${}^3D_{\pi\sigma}$  state dissociates easily to chemiluminescent products ( ${}^3n\pi^*$  excited and ground state carbonyl molecules) through the C–C bond cleavage. The simple analysis<sup>30</sup> is completely confirmed by MINDO/3 calculations<sup>29,31</sup>.

### 2.3. Photoisomerization and Fragmentation of Furans

The mercury ( $^3P_1$ )-sensitized isomerization of furans to cyclopropenyl ketones followed by decarbonylation (Fig. 3a) is a well known process<sup>25,32</sup>. We follow here the discussion given by Salem<sup>25</sup> for the singlet state correlation diagram (Fig. 3b). It is reasonable to assume that the primary reaction step is cleavage of a C–O bond to form a 1,5-diradical. As in the previous systems two different diradicals  $D_{\sigma\pi}$  and  $D_{\sigma\sigma}$  can be generated by the C–O bond cleavage (Fig. 3c). The former diradical correlates with the S and T  $\pi, \sigma^*$  excited states while the last one correlates with the ground singlet and T  $\pi, \pi^*$  excited state of furan<sup>25</sup>. The correlation is based on the electron count, which includes the two oxygen  $n$  electrons, the two  $\sigma$  electrons originally in the O–C<sub>2</sub> bond and the six  $\pi$  electrons of the furan ring (oxygen supplies two  $\pi$  electrons to the ring). Then furan has 4 $\sigma$ ,6 $\pi$  electrons, while  $\pi, \sigma^*$  excited state furan has 5 $\sigma$ ,5 $\pi$  electrons. Whereas the  $D_{\sigma\pi}$  diradical also has 5 $\sigma$ ,5 $\pi$  electrons it correlates with the  $\pi, \sigma^*$  excited state, the  $D_{\sigma\sigma}$  diradical has 4 $\sigma$ ,6 $\pi$  electrons and correlates with the ground singlet and with the lowest triplet  $\pi, \pi^*$  state of furan (the  $\pi$ – $\pi^*$  excitation does not change the number of  $\pi$  electrons). We can now explain the high efficiency of the spin-forbidden triplet  $\pi, \pi^*$  state-sensitized process of isomerization to the singlet ground state of the cyclopropenyl compound. The  $^1D_{\sigma\pi}$  diradical, which is strongly stabilized by a pentadienylic-type resonance, is a likely precursor for C<sub>2</sub>C<sub>4</sub> closure to cyclopropene-2-carboxaldehyde. The correlation diagram demonstrates a T–S crossing between  $\pi, \pi^*$  triplet and  $\pi, \sigma^*$  singlet states. The large SOC in this crossing region is a driving force for the process shown in Fig. 3a.

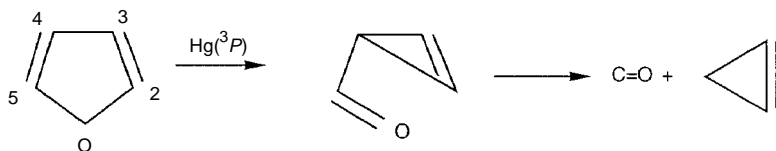
### 2.4. Spin–Orbit Coupling Effects in Reactions of Atomic Oxygen O( $^3P$ ) with Hydrocarbons

The first step of O( $^3P$ ) reactions with unsaturated hydrocarbons is a very rapid O( $^3P$ )-addition to the C=C double bonds. For olefins it corresponds to the triplet diradical production.

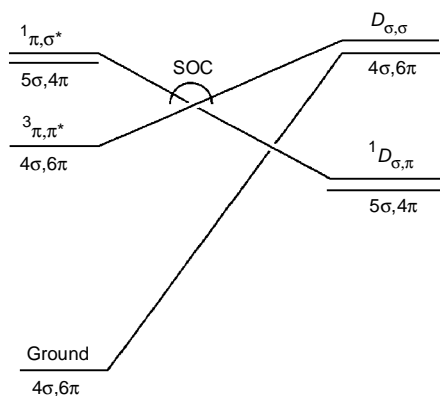


The final observed stabilized products are of two types: (i) oxiranes formed by ring closing of the diradical and (ii) aldehydes formed by the 1,2-shift of hydrogen in the diradical. The main feature of these processes is that ring closure of the triplet diradical and its rearrangement to aldehyde is spin-forbidden. The epoxides and aldehydes are closed shell molecules, so during the cyclization of the triplet diradical or the 1,2-hydrogen shift there must be a T–S transition. The idea of a competition between the T–S transition and other elementary processes in the diradical as a determining step in the

a



b



c

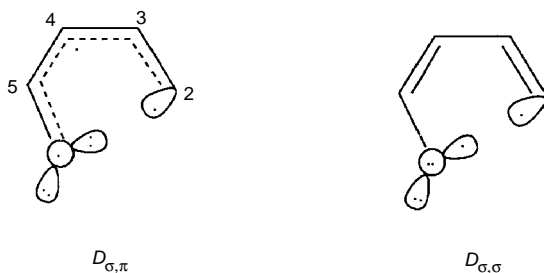


FIG. 3

Isomerization of furan to cyclopropene-2-carboxaldehyde: **a** the total photofragmentation of furan; **b** state correlation diagram for the C-O bond cleavage; **c** orbital structure of the 1,5-diradicals

reaction mechanism was proposed<sup>2</sup> on the basis of MINDO/3 CI calculations of reaction (2) with the account of SOC. All quantum chemical calculations show that there are four close-lying states in the diradical. Their electronic structures are represented in Fig. 4a. Each  $D$  state may be a singlet or a triplet. The qualitative potential energy surfaces (PES) for this reaction are given in Fig. 5. The triplet diradical  ${}^3D_{\sigma\pi}$ , initially formed in the first step of the reaction, can undergo intersystem crossing to the  ${}^1D_{\sigma\sigma}$  state because of the large SOC on the oxygen atom. The  ${}^3D_{\sigma\pi}$ - ${}^1D_{\sigma\sigma}$  transition includes the rotation of the  $2p$  AO on oxygen around the C-O bond which creates the torque to flip the electronic spin. The singlet  ${}^1D_{\sigma\sigma}$  diradical must produce the cyclization product (oxirane).

The T-S transition that occurs during the intramolecular 1,2-shift in the diradical can be explained by Fig. 4b. In this case the reaction starts from the  ${}^3D_{\sigma\sigma}$  state of the diradical. Removal of the H atom from the central carbon and its addition to the terminal carbon atom leads to formation of an intermediate diradical state,  ${}^3D_{\sigma\pi}$ . There is a crossing of the  ${}^3D_{\sigma\pi}$  and  ${}^1D_{\pi\pi}$  potential energy surfaces for the reaction coordinate. The

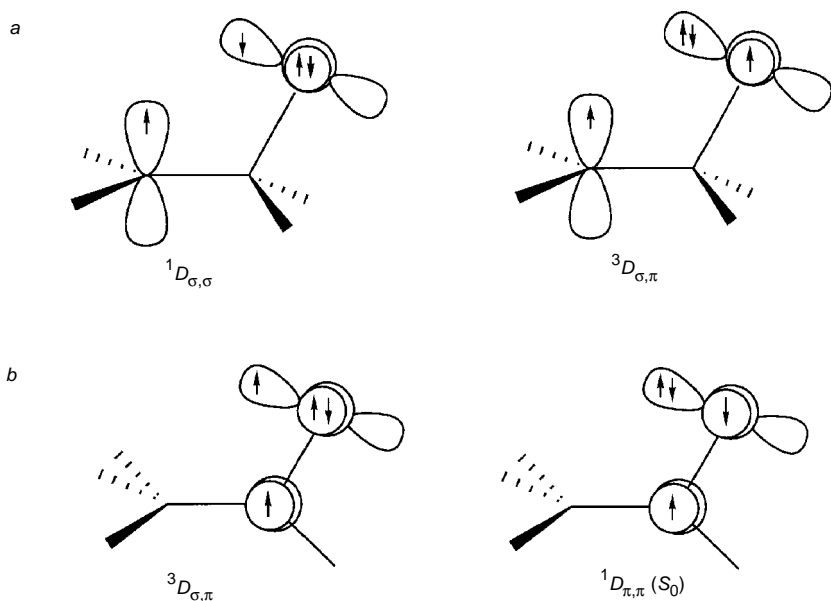


FIG. 4

Qualitative orbital structures for different states of diradicals: **a**  $\text{CH}_2\text{CH}_2\text{O}$  diradical produced in reaction (2) as a precursor of oxirane; **b**  $\text{CH}_3\text{CHO}$  diradical obtained by 1,2-H shift from the previous one. The labels  $\sigma\sigma$  and  $\sigma\pi$  describe the orientation of the unpaired electrons; the first character refers to the carbon electron, the second to the oxygen electron; the  $\pi$  orbital is represented by a circle

latter PES leads to the ground singlet state of the carbonyl. The  ${}^3D_{\sigma\sigma}-{}^1D_{\pi\pi}$  transition must be very effective, because of the orbital torque on oxygen "during" the ISC.

Another example of manifestation of SOC is given by the  $O({}^3P)$  reactions with aromatic hydrocarbons. The puzzling feature of these processes is the ability of the oxygen  $O({}^3P)$  atom to insert into C–H bonds. For example, in  $O({}^3P)$  reactions with benzene and toluene the phenol yield is 10 – 15%. Insertion reactions of a triplet atom in the C–H bond is obviously a spin-forbidden process and this forbidness is usually well fulfilled for saturated compounds. Let us consider the  $O({}^3P)$  reaction with benzene as illustration. It is well known that the first step of this reaction is an addition of the  $O({}^3P)$  atom leading to triplet diradical formation (Fig. 6a). This is not a stable intermediate; it pushes out the hydrogen atom, initially forming a triplet radical pair (RP) (see Fig. 6b). As the hydrogen atom is removed the residual part of the system becomes planar and obtains the structure of the phenoxyl  $\pi$  radical (see Fig. 6b). Recombination of this RP by phenol formation is impossible considering the spin and orbital forbidness (phenol is a planar molecule). Removal of the H atom is determined by exchange repulsion between the electrons with parallel spins on the O and H atoms. But the repulsion would be changed to attraction if the T–S transition occurs (Fig. 6c). The SOC matrix element for such an ISC process must be large, because of the rotation of the  $2p$  electron on oxygen accompanying the T–S transition (Fig. 6b – 6c). The ISC rate constant can effectively compete with a dissociation processes of the diradical, resulting in the observed yield of phenols. The high topicity of this reaction  $\sigma(\sigma,\sigma)$  and tightly bound RP (or diradicaloid) formation with  $T_{\sigma\pi}-S_{\sigma\sigma}$  crossing provide the effective T–S SOC mixing, making the reaction effectively allowed. However, high heterogeneous topicity

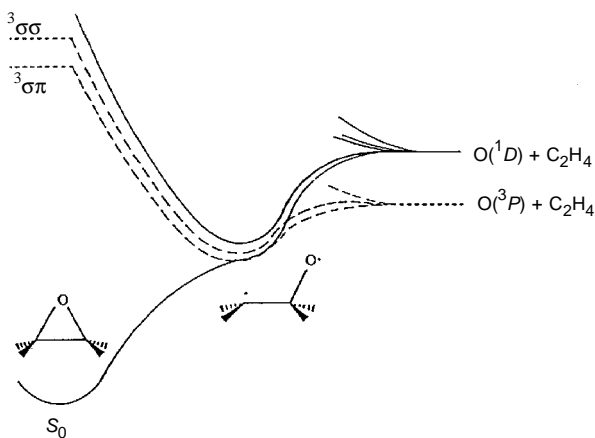


FIG. 5

Cross sections of qualitative potential energy surface along the reaction path of the  $O({}^3P)$  addition reaction to ethylene

of the intermediate diradical can not guarantee an effective ISC process in a chemical reaction. Instructive example of this are provided by the reactions of molecular oxygen<sup>2</sup>.

### 2.5. Spin-Orbit Coupling Effects in Reactions of Molecular Oxygen with Unsaturated Hydrocarbons

In the ground triplet channel of molecular oxygen reaction with ethylene<sup>2</sup>, there is an involvement of a 1,4-diradical as an intermediate. The formation of the 1,4-diradical  $\text{CH}_2\text{CH}_2\text{O}\dot{\text{O}}$  as a primary process has been obtained in MINDO/2  $3 \times 3$  CI calculations for the ground state triplet PES ( $^3A''$ ) and for one component of  $a^1\Delta_g$  state of same spatial symmetry ( $^1A''$ ) (see Fig. 7 and ref.<sup>4</sup>). The CCOO plane has here been assumed as an effective element of symmetry in a first simplified approach. The orbital structure of both states and their reaction paths are very similar; in the 1,4-diradical stage they are approximately degenerate. The other component of  $a^1\Delta_g$  state symmetry ( $^1A'$ ) also passes through the quasidiradical path, but does not form a physically stable diradical minimum; the  $^1D_{\sigma\sigma}$  is unstable relative to cyclization into dioxetan<sup>2</sup>. The geometry optimization of the reaction path produces some deviations out of the CCOO plane for the terminal oxygen, so a complicated interference of the two singlet channels occurs, producing a quasidiradical mechanism of the singlet  $a^1\Delta_g$  oxygen cycloaddition reaction with olefins<sup>2</sup>. The main feature of the triplet molecular oxygen reactions with unsaturated hydrocarbons is that these processes are effectively forbidden by spin selection rules, in contrast to the atomic  $\text{O}(^3P)$  reactions; the SOC between T and S states in the  $D_{\sigma\pi}$  diradical  $\text{CH}_2\text{CH}_2\text{O}\dot{\text{O}}$  is equal to zero (or very small), because of the same orbital structure of the two states. We can expect similar types of intermediate diradicals in  $\text{O}_2(X^3\Sigma^-)$  reactions with dienes and aromatics. So the T-S transitions in reactions of molecular oxygen with unsaturated hydrocarbons are strictly forbidden

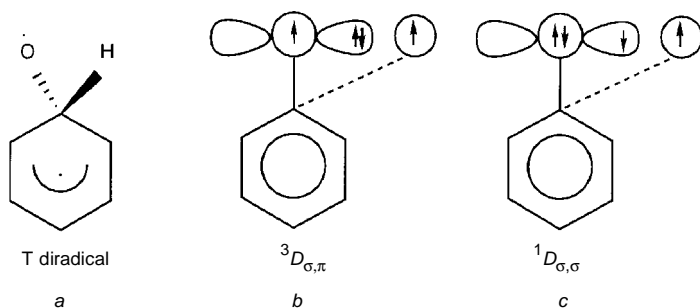


FIG. 6

Orbital structures of intermediate stages of the reaction:  $\text{O}(^3P) + \text{benzene} \rightarrow \text{phenol}$

(otherwise our world would be burnt). Inclusion of  $d$  orbitals of the metal catalyst can introduce different orbital structures for S and T states with non-zero SOC matrix elements such that the S–T transition becomes chemically competitive during the catalytic action. We know that catalytic insertions of  $O_2$  into organic substrates are involved in the synthesis of many metabolic products. These processes should be the subjects of spin-catalysis. In general, if the S–T transition in a symmetry forbidden reaction does not satisfy the above mentioned requirements and is not effectively allowed by the intrinsic SOC, the catalyst inclusion is necessary in order to promote the spin forbidden reaction.

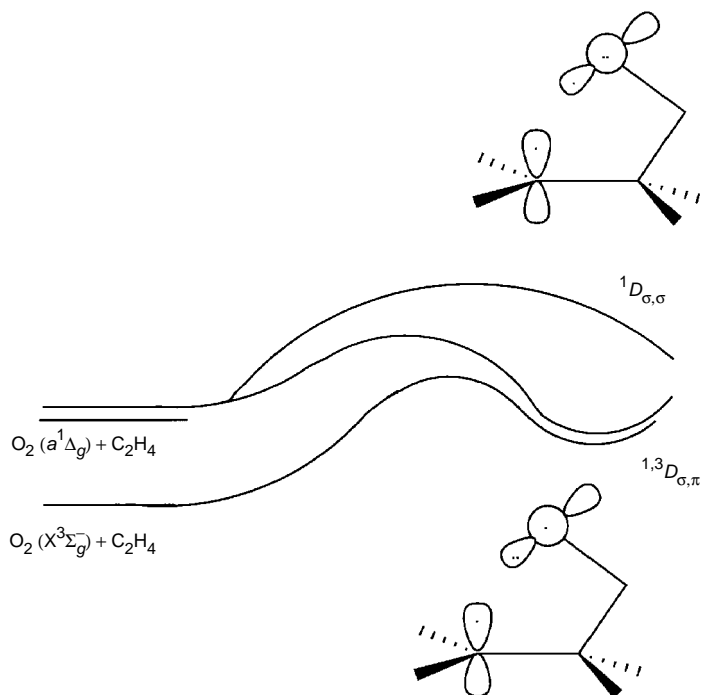


FIG. 7

Cross sections of qualitative potential energy surface along the reaction path of the  $O_2(^3\Sigma_g^-, ^1\Delta_g)$  addition reaction to ethylene with diradical formation  $CH_2CH_2OO$

### 3. THE MECHANISM OF THE EXTERNAL HEAVY ATOM SPIN-CATALYSIS

The SOC induced spin-catalytic processes are known in photochemistry as an external heavy atom (EHA) effect on product ratios and on quantum yields<sup>17,33</sup>. For a proper understanding of the EHA spin-catalysis mechanism we must consider first a simple physical model of the EHA effect on S–T transitions in unsaturated hydrocarbons. Forty years ago Kasha discovered the spectroscopic EHA effect by observing a yellow colour that developed by mixing two colourless liquids, chloronaphthalene and ethyl iodide<sup>34</sup>. Kasha showed that the colour was due to an increase of probability for the S–T absorption of the aromatic molecule. It has been confirmed that the EHA effect originates in SOC and that it grows in magnitude with the strength of the acid–base interaction between the aromatic donor and the alkyl halide acceptor<sup>22</sup>. The EHA effect on nonradiative S–T photophysical processes has also been studied<sup>22,35</sup>. Very often the same pure physical mechanism operates in the EHA spin-catalysis. The involvement of EHA-induced SOC effects into the photochemical transformation on the intermediate stage of the process has also been proposed<sup>33</sup>. Such effects should be most important in homogeneous catalysis by transition metal compounds<sup>17</sup>. In order to understand the mechanism of SOC induced spin-catalysis we must start with the simplest physical model of the EHA effect on singlet–triplet radiative transitions.

According to the general discussion in the monograph of McGlynn et al.<sup>22</sup> there are two main types of interpretations of EHA, resting on exchange<sup>36</sup> and charge transfer<sup>37</sup> type mechanisms, respectively. Recently the EHA effect on the  ${}^3\pi\pi^* \leftarrow S_0$  vertical transition in a planar ethylene molecule was studied for collision complexes between ethylene and halogen anions as a simple physical model for the spin-catalytic action<sup>38</sup>. The analytic multi-configuration quadratic response (MCQR) theory with the complete Breit–Pauli form of the SOC operator was used in these calculations<sup>38,39</sup>. For the free ethylene molecule almost the whole intensity of the vertical  $T_1 \leftarrow S_0$  transition (98%) was obtained as polarized perpendicular to the molecular plane. This intensity is determined by transitions to the  $T^y$  spin sublevel, where  $y$  is the in-plane axis perpendicular to the C=C bond. The transition moment is equal to  $6.31 \cdot 10^{-5}$  a.u. which corresponds to an oscillator strength of  $f = 4 \cdot 10^{-10}$ . The calculated EHA spin-catalysis of this transition rate shows that all anions are effective as external heavy atoms at short distances of collision ( $4 \text{ \AA}$ ) and that the  $T_1 \leftarrow S_0$  intensity enhancement strongly depends on the nuclear charge of the EHA. For the  $F^-$ ,  $Cl^-$  and  $Br^-$  complexes the calculated oscillator strength of the T–S transitions in ethylene is calculated to be  $2.9 \cdot 10^{-9}$ ,  $1.2 \cdot 10^{-8}$  and  $1.1 \cdot 10^{-6}$ , respectively. The spin-catalysis works as an enhancement of the internal magnetic interactions inside the ethylene moiety because of charge transfer (CT) admixtures of different orbital symmetry to the T and S states. The SOC matrix elements in free ethylene are smaller than  $20 \text{ cm}^{-1}$ . In the collision complex of ethylene and  $Cl^-$  the SOC matrix elements exceed this maximum value by few times<sup>38</sup>. There are numerous new contributions from the CT states and from the states of mixed character.



Charge transfers from different  $p$  lone pairs of halogen have different orbital symmetry and produce admixtures to T and S states of ethylene in such a way that a great enhancement of T–S transition is induced. For example, the CT  $p_z(X) \rightarrow \pi_{C=C}^*$  admixture to the singlet state and the admixture of the CT configuration  $p_x(X) \rightarrow \pi_{C=C}^*$  excitation to the triplet state produce a large one-center SOC contribution to the S–T transition rate. This SOC could not be obtained by direct two-centre integrals  $\langle p_z(X) | \mathbf{H}_{SO} | \pi^* \rangle$ , because they are negligible at a large distance for EHA ( $r = 4 \text{ \AA}$ ). Mixtures of MO LCAO coefficients are also rather small at this large distance and the main contribution to the SOC  $\langle S_0 | \mathbf{H}_{SO} | T_2 \rangle$  element is determined by the CI admixture of the  $^1CT_x$  and  $^3CT_z$  to the  $S_0$  and to the  $T_2$  states, respectively. This introduces the one-centre SOC integral contributions<sup>40</sup>. The number of new low-lying CT states (charge transfer from  $p_x$  and  $p_z$  orbitals of halogen to  $\pi^*$  MO of ethylene) and the increased SOC serves as indications of an EHA effect. The charge transfer from different quasidegenerate  $p$  orbitals of the halogen catalyst introduces the orbital angular momentum shifts into the singlet and triplet states of the ethylene molecule (catalysant). The singlet–triplet states perturbation by SOC is very sensitive to such a small intermolecular deformation of the electronic shell. Slight CT admixtures of anisotropic character produce an important magnetic perturbation in the catalysant which is responsible for the enhancement of the S–T transitions. The same type of analysis could be applicable for photochemical processes and even for dark reactions. For examples, the photochemical reduction of 2,2'-pyridyl (di-2-pyridyl diketone) to the *cis*-enediol compound (*cis*-1,2-di(2-pyridyl)-1,2-ethenediol) in ethers is changed by the EHA effect (the addition of 1,2-dibromoethane) to the production of the *trans*-enediol<sup>41</sup>. The 1,2-dibromoethane with concentration of  $10^{-3} \text{ mol/dm}^3$  works as a selective spin-catalyzator of *trans*-enediol formation and depresses the yield of the *cis* product. This has been interpreted as an enhancement of the intersystem crossing efficiency from the lowest excited S state to the lowest T state of 2,2'-pyridyl and as a difference in the S and T state photochemical reactivity<sup>41</sup>. But qualitative analysis of potential energy surfaces and search of the reason for the difference in the S and T state reactivity show that EHA can be involved on the intermediate stage of hydrogen abstraction and radical pair formation. A similar EHA effect on the efficiency of isomerization of the thiocarbocyanine dye in a frozen medium is known<sup>42</sup>. The addition of ethyl iodide increases the rate of isomerization far more than does addition of an equivalent amount of ethyl chloride. A lot of other examples of the same type of EHA spin-catalysis are available<sup>17,33</sup>, including important biochemical applications<sup>43,44</sup>.

Direct involvement of charge-transfer steps in chemical processes leads to more prominent EHA spin-catalysis. The time-resolved study of the EHA effect on the photochemistry of a cyanine iodide ion pair reported in ref.<sup>45</sup> gives one of several interesting examples. It was shown that the EHA effect on cyanine dyes may influence their behaviour as sensitizers in photographic processes. In this application the dyes are ab-

sorbed onto the surface of silver halide crystals. Other examples of the EHA spin-catalysis of electron-transfer reactions and radical yields are also known<sup>17,46–48</sup>. The free-radical yield decreases extremely much on substituting a heavy atom into the triplet quenchers<sup>46</sup>. It was shown that the EHA effect is caused by SOC between the triplet state of the geminate radical pair and the singlet ground state of the neutral D–A pair of molecules<sup>46,48</sup>. This mechanism of the EHA spin-catalysis has been the subject of theoretical interest for a long time<sup>20,40,49–65</sup>. It was theoretically predicted for *para*-halogenated nitrobenzene reaction with hydroxyl anion on the ground of INDO calculations with account of SOC (ref.<sup>66</sup>). Though the INDO method predicts an artificial barrierless potential for the OH<sup>−</sup> addition to nitrobenzenes (NB), the qualitative features of SOC integrals seem to be reliable. The HOMO–LUMO interaction for the donor (OH<sup>−</sup>) and acceptor (NB) orbitals govern the SOC matrix element between ground singlet and charge transfer triplet states. The tightly bound  $\pi$ -complex in the ground triplet charge-transfer state could be obtained after the ISC process on the first stage of the addition reaction; it should work as a triplet trap in the reaction and initiate radical chain process, which are well known for such systems<sup>66</sup>.

The triplet mechanism of external magnetic field effects on radical yields should serve as a useful test of spin-catalysis by EHA (refs<sup>15,59</sup>). This mechanism depends on selective ISC rates from different spin sublevels of the zero-field splitting (ZFS) in reactive triplet state. Since the Zeeman interaction is randomly oriented complexes mixes the ZFS spin substates, the ISC selectivity is averaged out during one Larmor period with the effect that the overall intersystem crossing rate increases<sup>15</sup>. A characteristic feature of the triplet mechanism is that the MF effect saturates at high fields when the Larmor frequency exceeds the spin-lattice relaxation and the ISC rate constants<sup>59</sup>. Because the EHA effect is highly spin anisotropic<sup>38,40</sup> the EHA spin-catalysis rate would be quite sensitive to the external magnetic field, if the triplet mechanism of MF effect is reliable. Examples of such spin-catalysis in photophysical reactions in liquid and solid solutions are quite numerous<sup>15,21, 54,55,60,62–64,67–69</sup>. One of the most interesting examples is the EHA spin-catalysis of triplet–triplet annihilation reactions<sup>67</sup>. Competitive influence of magnetic field and EHA on the annihilative delayed fluorescence of anthracene and rhodamine 6G in solutions revealed a spin-catalytic nature of the EHA effect in this reaction<sup>2,54,68</sup>. The simplest phenomenological explanation of this effect was a proposition that EHA influences the zero-field splitting parameters of aromatic triplet molecules<sup>2</sup>; the ZFS parameters enter into the theory for the MF effect on T–T annihilation<sup>70</sup> and the EHA dependence of this magnetic field-induced spin-catalysis could be explained in a framework of the theory of Atkins and Evance<sup>17</sup>. More detailed explanation includes the direct quantum chemical calculation of the SOC anisotropy in triplet states of collision complexes<sup>2,38,40,61</sup>. Calculations of model complexes of ethylene with different external heavy atoms show the strong EHA effect on spin-lattice relaxation (SLR) in the lowest triplet state of ethylene molecule through CT

admixtures<sup>2</sup>. Triplet CT states of three different symmetries, which are produced by charge transfer from  $p_x$ ,  $p_y$  and  $p_z$  EHA orbitals, give different admixtures by intermolecular configuration interaction to the ethylene triplet ( $T_1$ ) state. Strong SOC between these CT states produces in the second order of perturbation theory an intensive mixing of ZFS spin sublevels of the ethene  $T_1$  state. The effect is strongly dependent on the geometry of collision. Therefore, the intermolecular Coulomb interaction in a tight collisions with EHA can influence the SLR rate in  $T_1$  state of unsaturated hydrocarbons<sup>2</sup>. The increase of SLR rates cause the enhancement of triplet–triplet annihilation. The recent *ab initio* calculations<sup>38</sup> fully confirm the old MINDO/3 CI SOC predictions<sup>2,61</sup>.

#### 4. SPIN-CATALYSIS BY TRANSITION METAL COMPOUNDS

Chemical reactions catalyzed by transition metal compounds constitute the main body of catalysis phenomena involved in major industrial processes. Transition metal complexes can change their own spin multiplicity during monomolecular rearrangements (spin-crossover)<sup>71</sup>. The involvement of multiplicity changes in chemical processes catalyzed by these compounds, has also been revealed<sup>5,6,72</sup>. The study of connections between intramolecular spin-crossover and catalytic action is one of the most important aspects of spin-catalysis theory. These connections could be determined by both of the two main types of spin-catalysis. Low spin and high spin multiplets in the metal complex normally have different orbital symmetry and different ability to perturb organic substrates by exchange interaction. If the spin transition is localized on the organic substrate the assistance of the  $d$ -metal ion could be realized in the SOC enhancement and in the lowering of the activation energy by transition through the S–T crossing point. The role of spin crossing in such thermal processes could be revealed by an application of an external magnetic field. Interesting catalytic thermal reactions have been studied by Perito and Corden in external magnetic field<sup>73</sup>. An applied magnetic field alters the oxidation rate of 2,6-di-*tert*-butylphenol (DTBP) to the corresponding benzoquinone in the presence of O<sub>2</sub> and a transition metal catalyst, cobalt(II)bis(3-(salicylideneamino)propyl)methylamine. The dependence of the relative reaction rate on the MF strength is analogous to the MF effect on photochemical  $\alpha$ -cleavage of cycloalkanones, considered above in Section 2.1., where the MF alters the ISC rate between a triplet radical pair and a singlet state product<sup>18</sup>. The relative rate ( $k_r$ ) is the ratio of the reaction rate at magnetic field ( $H$ ) to the rate at zero field. The observed dependence of  $k_r$  is between a maximum value of 1.6 in a weak field ( $H = 0.1$  T) and a minimum value of 0.8 in a vary high magnetic field ( $H = 7$  T). The relative contribution of SOC and hyperfine coupling to intersystem crossings has been determined, assuming that the radical pair reaction is responsible for the observed magnetochemistry and following the procedure developed by Doubleday and Turro<sup>18,73</sup>. The SOC contribution was estimated to be higher at all fields. The cobalt-catalyzed oxidation of DTBP consists of five steps; few of them include the phenoxy radical intermediate. The rate deter-

mining step is represented in Fig. 8b which was chosen from a detailed analysis of the MF effect<sup>73</sup>. This is a catalyst regeneration reaction and it can alter the total reaction rate by changing the steady-state concentration of the phenoxy radical. The potential energy curves for the O–H bond dissociation in phenol<sup>74</sup> is qualitatively represented in

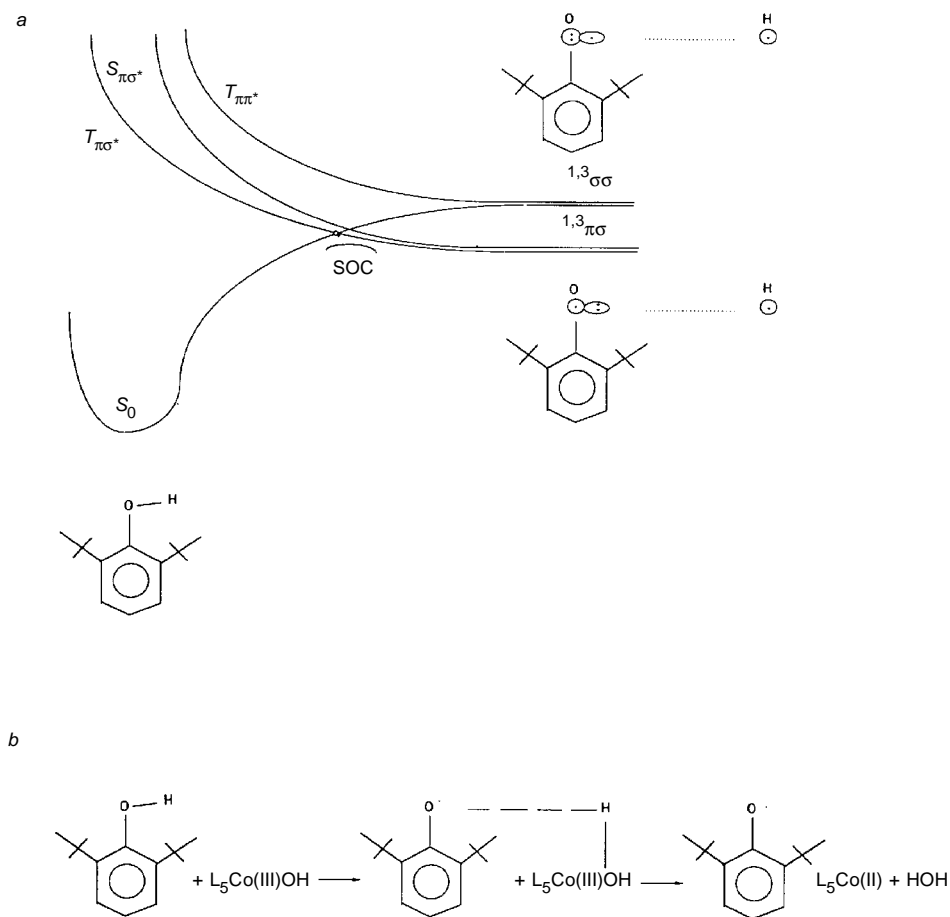


FIG. 8

The rate determining (spin-catalytic) step in catalytic thermal oxidation of 2,6-di-*tert*-butylphenol to the 2,6-di-*tert*-butylbenzoquinone in the presence of cobalt(II)bis(3-(salicylideneamino)propyl)methylamine and  $O_2$ . **a** Potential energy curves and orbital correlation diagrams illustrating the S–T transition during the O–H bond rupture in butylphenol. **b** The rate determining step; all other steps and details of the total mechanism are given in ref.<sup>73</sup>

Fig. 8a. It is again accounted for in Fig. 8a. As in the case of the  $O(^3P)$  reaction with benzene (Fig. 6), the phenoxyl is a  $\pi$  radical in the ground state and its  $n \rightarrow \pi$  excited state is higher<sup>74</sup> in energy by 0.8 eV. It means that during a radical pair formation reaction the S–T crossing must occur with large, highly anisotropic, SOC induced on the oxygen atom. This is because the S–T transition includes the orbital rotation on oxygen, which produces an orbital angular momentum which interacts with the spin, thereby providing the torque<sup>3,74</sup>. This orbital rotation involved in S–T transitions in analogous to the large SOC matrix element between charge transfer states in the ethylene +  $Br^-$  complex. The S–T transition in the crossing region explains the observed magnetic field effect in this catalytic reaction. Participation of a Co atom in this magnetic perturbation is obvious because of its involvement in the hydrogen transfer process; we can suspect that the activation energy of this process (S–T crossing point in Fig. 8a) should be diminished by the transition metal  $d$  orbital participation. Therefore we can suspect that the cobalt atoms also can enhance SOC in this effectively allowed S–T intercombination crossing.

#### 4.1. Intersystem Crossing Localized at the Transition Metal Site

Spin equilibria in biomolecules were first reported in 1937, when Pauling et al. observed that an increase of pH reduced the magnetic moment of ferric hemoproteins<sup>75</sup>. Since that time a huge amount of studies have been devoted to the problem of a thermal equilibrium between high spin and low spin species (see e.g. refs<sup>6,71,72,76</sup>). It has been established that only slight modifications of axial ligands are sufficient to induce a spin crossover in hemoproteins<sup>72</sup>. Spin transitions occurring at metal sites in proteins can be rate controlling in the functioning of certain metalloenzymes<sup>6</sup>. Studies of the dynamics of the spin changes in metalloproteins in a wide range of solvents suggest that the spin crossover is accompanied by a rearrangement of the protein moiety so as to imply a “functional role” of the spin equilibrium. The occurrence of the spin change should help electron transfer in redox processes. Actually, many metalloproteins in which spin equilibria are found are involved in enzymatic oxidation-reduction reactions<sup>72</sup>. Analysis of the electron-transfer rate data reveal a linear free energy relationship between the activation energy for the first electron-transfer event for the redox couple of cytochrome P-450 with an iron-sulfur protein (putidareoxin) from one side, and the spin equilibrium free energy, from the other side<sup>6</sup>. Cytochrome P-450 is the ultimate electron electron acceptor of a soluble electron-transfer protein chain. Upon binding the natural substrate camphor, the maximum of the Soret absorption of cytochrome P-450 is significantly blue shifted. This shift is due to intersystem crossing from low spin ( $S = 1/2$ ) ferric iron to high spin ( $S = 1/2$ ) iron of the porphyrin system. The reduction potential for P-450 becomes significantly more positive when the camphor substrate binds and electron transfer occurs<sup>6</sup>. So these natural systems are created for spin-catalysis in live matter. The conformational changes induced by spin transitions were found

responsible for oxidative phosphorylation catalyzed by enzymes<sup>77</sup>. Conformational changes and spin changes are undoubtedly related to each other and such links are significant for the enzymatic activity<sup>72</sup>.

The importance of transition metal centers as catalysts has prompted extensive studies of transition metal ion reactions in the gas phase by modern mass spectrometric techniques (ICR, REMPI)<sup>78</sup>. By these state-specific studies unambiguous observations of SOC-induced nonadiabatic behaviour in metal ion reactions have been obtained, for example in the reactions of  $\text{Fe}^+(^6D, ^4F)$ ,  $\text{V}^+(^5D, ^3F)$  with  $\text{H}_2$ , water, methane and ethane<sup>78</sup>. The spin-prohibition is overcome in the preliminary step of the transition metal involvement into the catalytic process (activation of the H–H and C–H bonds). We can suspect that this catalyst spin-activation should be a wide-spread phenomenon in catalytic processes. In general, transition metal-oxide species are important in catalysis. They have been used to convert alkanes to alcohols, the processes that are of great industrial interest. The mechanism proposed to explain these catalytic reactions involves formation of metal-hydroxide intermediates<sup>79</sup>  $\text{R–M–OH}$ , though little is known about the detailed steps associated with these processes. The reaction of nickel atom with water in the gas phase has been investigated recently by kinetic spectroscopy and *ab initio* methods<sup>80</sup>. The triplet ground state nickel atom produces first a weakly bound molecular complex with water (7.2 kcal/mol). At the complex well there is also a well on the excited singlet state surface, which is only 3.4 kcal/mol higher. The triplet surface has a very high barrier for the insertion into the O–H bond and for the production of triplet ground state nickel hydroxide  $\text{H–Ni–OH}$ , but the barrier for the singlet state reaction channel is rather small<sup>80</sup>. There are strong kinetic and theoretical arguments that the reaction occurs by  $T \rightarrow S$  intersystem crossing on the stage of the weak  $\text{Ni}\dots\text{H}_2\text{O}$  complex. The singlet channel correlates with the excited state  $(d^9s^1)^1D$  nickel atom for which the barrier for oxidative addition is low, because the  $3d$  and  $4s$  orbitals can hybridize away from the water molecule and thereby allow water to approach close enough to Ni and to produce the insertion. At the transition state the  $d$  population is 9.01 and the nickel charge is  $-0.09$ , showing that the leading atomic state of nickel is the  $d^9s^1$  state. Unlike the case of the singlet surface where the bonds are  $sd$  hybrids, the bonds formed on the triplet surface are  $sp$  hybrids<sup>80</sup>. It means that a large orbital angular momentum shift can be induced during the  $T$ – $S$  transition and therefore a large SOC matrix element  $\langle a_{ST} \rangle$  could be expected. By these simple arguments we can explain the SOC induced  $T \rightarrow S$  ISC in the entrance channel of  $\text{Ni} + \text{H}_2\text{O}$  reaction and the effective  $S \rightarrow T$  relaxation in the insertion product  $\text{HNiOH}$ . Because of the involvement of such type intermediates in important catalytic processes<sup>79</sup> we can consider this as an example of SOC induced spin-catalysis.

Other examples are also available. Cross sections for the reactions of  $\text{Fe}^+(^6D, ^4F)$  with  $\text{D}_2\text{O}$  have been studied recently<sup>81</sup> by guided-ion beam tandem mass spectrometry. A similar conclusion about more reactive  $^4F$  excited states in the insertion reaction to

form a  $D-Fe^+-OD$  intermediate has been obtained from this state-specific study. A high efficiency of spin-forbidden processes has been proved for many ion-beam reactions<sup>78</sup>. Quite interesting observations concern the reaction of  $Fe^+$  ion with  $O_2$ ; the  $^4F$  excited state is only two times more reactive than the ground state  $^6D$ . This is in sharp contrast to the relative reactivities of these states observed for reactions with closed shell molecules ( $H_2$ , alkanes), which are by factors of 10 – 100 larger<sup>78</sup>. Adding two unpaired electrons to the  $O_2$  molecule changes the total spin of the system and effectively mixes the reactant states  $Fe^+(^4F, ^6D)$  by intermolecular exchange interactions in the transition state region. Considering such a reaction as a model for a preliminary step of catalytic oxidation process, we can treat it as a spin-catalysis of the second type, or as a combination of I and II types of spin uncoupling processes.

#### 4.2. Spin-Photocatalysis

Some examples of SOC-induced intersystem crossings providing activation of chemical changes can be tentatively found in heterogeneous photocatalysis. Upon photoexcitation of a number of semiconductors nonhomogeneously suspended in solutions or in gases, simultaneous oxidation and reduction reactions occur<sup>82</sup>. These reactions involve photosensitization, i.e. energy transfer or reversible electrone-hole transfer from a semiconductor particle, which often is stable to irradiation of light and acts as the photocatalyst during a large number of oxidative conversions per active site without degradation. This field was prompted by the discovery of water splitting upon illumination of a  $TiO_2$  electrode<sup>83</sup> and is now widely extended as a means of solar energy conversion. In general, in doped semiconductors the impurity centres can be formed, like the Si-S1 centre in silicon<sup>84</sup>. The anisotropy of magnetic field effects on photoconductivity and electron-hole recombination in such semiconductors reveal the importance of SOC effects<sup>84</sup>. Unlike metals, semiconductors lack a continuum of interband states to assist the recombination of the electron-hole pair. This assures an electron-hole pair lifetime sufficiently long to allow these species to participate in interfacial electron transfer and subsequently be capable to initiate redox processes with surface-adsorbed organic molecule<sup>82</sup>. The SOC in the electron-hole pair can induce the S-T transitions preventing the further recombination by the spin-selection rule. Participation of metal  $d$  orbitals in the hole formation could enhance the SOC matrix elements in the same manner, like in the above considered example of halogen  $p$  orbitals involvement in charge-transfer states of different spin and orbital symmetry (Section 3).

The spin-catalysis with inhibition of radical formation in photoelectron transfer reactions on surfaces is now known from studies by magnetokinetic methods<sup>62-64,85,86</sup>. In the pioneering work by Kiwi<sup>85</sup> the Ru-trisbipyridyl and methylviologen ( $MV^{2+}$ ) system was used to sensitize  $H_2$  evolution at the surface of semiconductors particles. The observed magnetic field effect on the rate of hydrogen production was attributed to radical recombination processes on the surface<sup>85</sup>. The recent research by Steiner et al.<sup>86</sup>

have shown that the mechanism of the MF effect is more complicated and depends on SOC perturbation. The efficiency of free radical formation of  $MV^+$  is quite small, indicating a large efficiency of fast backward electron transfer. The photoreactive state of the  $Ru(bpy)_3^{2+}$  ion is a metal-ligand charge transfer triplet state. The primary redox pair has also triplet spin correlation and the backward electron transfer (quenching to the  $S_0$  ground state) is spin-forbidden<sup>86</sup>. But we can suspect from previous analysis (Section 3) that this redox pair recombination with quenching to the stable closed shell ground state will be induced by a non-zero SOC matrix element. The yield of  $MV^+$  radicals decreases with increasing magnetic field which can be explained in terms of MF-enhanced backward electron transfer in the primary redox pair<sup>86</sup>. The energy separation between the singly-occupied frontier molecular orbitals, resulting from a weak trigonal ligand field splitting of the Ru 4d-AO, is rather small. These quasidegenerate MO's produce different charge transfer states of both multiplicities with large SOC matrix elements in accordance with the above mentioned analysis of the EHA effect. In primary redox pairs the large SOC and near-degeneracy of few different CT states, including different 4d orbitals, will lead to large differences of the triplet spin sublevels properties; their singlet state admixtures and the rates of the backward electron transfer will be quite different. A magnetic field mixes the spin sublevels and enhances the quenching of the primary redox pair. This is an example of competition between the chemical SOC-induced spin-catalysis and a negative spin-catalysis induced by a magnetic field effect. The last catalysant of pure physical nature (MF) influences the chemical reaction (the yield of radicals  $MV^+$ ) and helps to reveal the role of intrinsic magnetic perturbation (SOC) in chemical reactivity.

Since the whole system, Ru-trisbipyridyl + methylviologen, involved in photocatalysis of hydrogen production from water, we can propose that such combined studies of spin-catalysis phenomena have to be undertaken for many other similar systems. Till now, studies of the influence of a magnetic field on heterogeneous catalysis are scarce<sup>85,87</sup>. The enrichment of magnetic isotopes in photolysis of dibenzyl ketones and benzoyl peroxides are the simple examples of spin catalysis induced by hyperfine electron-nuclear coupling in radical pairs with a clear nature of a magnetic field effect on this process<sup>88</sup>. In spite of the practical importance of magnetic isotope enrichment<sup>88</sup> we must stress that the radical pair theory could not be the only guideline in spin-catalysis. This is rather a side branch of relatively minor importance, though the MF effects in chemical reactions often are interpreted in a framework of RP theory<sup>16</sup>. Applications of magnetic fields in catalysis by transition atom compounds<sup>5,85,89</sup> reveal the importance of SOC-induced magnetosensitive steps, which, however, are not consistent with the radical pair theory. We hope that further investigations of MF effects in catalysis will shed more light on this problem.

The photochemistry of transition metal compounds has also been used to generate very active intermediates in many catalytic processes<sup>90</sup>. For instance, the photochemi-



cally induced elimination of hydrogen from hydride metal complexes produces unsaturated metal-containing intermediates able to activate the carbon–hydrogen bonds in aliphatic hydrocarbons. As pointed out by Megehee and Meyer<sup>91</sup>: “This extensive photochemistry has generally been based only on product and quantum yield studies. There is little insight in this area into excited-state dynamics, detailed photochemical mechanisms, or the nature of the excited states responsible for the photochemistry”. Quite recently potential energy curves from MCSCF CAS calculations have been reported for the homolysis of the metal–hydrogen bond in HCo(CO)<sub>4</sub> and HMn(CO)<sub>5</sub> photodissociations<sup>92,93</sup>. It is possible to propose that the ISC processes during the M–H bond cleavage are responsible for the dissociations which produce the active catalysts. Photolysis of the Mn–H bond in HMn(CO)<sub>5</sub> occurs upon irradiation at 51 800 cm<sup>-1</sup>. Calculations indicate that the singlet state corresponding to the  $\sigma \rightarrow \sigma^*$  excitation lies at much higher energy<sup>93</sup>. Veillard<sup>92</sup> proposed the mechanism for the photolysis of the metal–hydrogen bond in HCo(CO)<sub>4</sub>, which considers that excitations to the <sup>1</sup>E state corresponding to the  $d_\delta \rightarrow \sigma^*$  configuration is followed by intersystem crossing to the <sup>3</sup>A<sub>1</sub>( $\sigma \rightarrow \sigma^*$ ) state and subsequent dissociation to the products along the <sup>3</sup>A<sub>1</sub> curve. The recent CASSCF+MRCI calculations by Daniel<sup>93</sup> of HMn(CO)<sub>5</sub> photodissociation show the similar mechanism. The Mn–H bond homolysis with irradiation at 193 nm proceeds through the  $c^1E(d\pi \rightarrow \pi^*)$  state excitation followed by the intersystem crossing into the  $b^3A_1(\sigma \rightarrow \sigma^*)$  state at a stretched metal–hydrogen distance. An avoided crossing between the two <sup>3</sup>A<sub>1</sub> states leads by internal conversion to the  $a^3A_1(3d \rightarrow 4d)$  state with final dissociation along the <sup>3</sup>A<sub>1</sub>( $\sigma \rightarrow \sigma^*$ ) curve. In both these cases<sup>92,93</sup>, the <sup>3</sup>A<sub>1</sub>( $s \rightarrow \sigma^*$ ) dissociative curve is reached after intersystem crossings from a near-by singlet state <sup>1</sup>E. The <sup>1</sup>A<sub>1</sub>( $\sigma \rightarrow \sigma^*$ ) state does not play any role in these mechanisms, since it is a high-lying state (7.5 eV) as a consequence of its ionic character<sup>92</sup>.

It should be mentioned that SOC between the <sup>1</sup>E and <sup>3</sup>A<sub>1</sub> states is allowed in the C<sub>3v</sub> and C<sub>4v</sub> symmetry. The strong configuration interaction between ( $\sigma \rightarrow \sigma^*$ ) and ( $3d \rightarrow 4d$ ) configurations of <sup>3</sup>A<sub>1</sub> type<sup>93</sup> is very important for enhancement of the SOC matrix elements in the HMn(CO)<sub>5</sub> system, because this is the only way to induce a large orbital angular momentum shift during the ISC transition. Otherwise the SOC between the pure <sup>1</sup>E( $d \rightarrow \pi^*$ ) and the <sup>3</sup>A<sub>1</sub>( $\sigma \rightarrow \sigma^*$ ) configurations should be equal to zero because the two states have no orbitals in common<sup>94</sup>.

The SOC matrix element in HCo(CO)<sub>4</sub> between <sup>1</sup>E( $d-\sigma^*$ ) and <sup>3</sup>A<sub>1</sub>( $\sigma-\sigma^*$ ) states<sup>92</sup> should be non-zero because it includes some orbital rotation on the Co atom. Both states differ by *d* and  $\sigma$  MO's occupation; the  $\sigma$  orbital is delocalized around the Co–H bond so it includes some  $d_\sigma$  character on the cobalt atom. During the <sup>1</sup>E  $\rightarrow$  <sup>3</sup>A<sub>1</sub> ISC transition some part of  $d_\delta \rightarrow d_\sigma$  orbital rotation occurs which create a torque for the magnetic spin flip. The possibility of intermediate <sup>1</sup>E–<sup>3</sup>E intersystem crossings followed by the fast internal conversion <sup>3</sup>E–<sup>3</sup>A<sub>1</sub> could not be excluded, because in this case the completely localized rotation on the cobalt atom should induce the maximum

possible SOC matrix element  $\langle a_{ST} \rangle$ . Anyway we can see an effective possibility for the ISC dissociative path, which includes the  $S \rightarrow T$  nonadiabatic transition.

These processes could be considered as a photoactivation of the catalyst and as the first type of spin-catalysis induced by large SOC originating at the transition metal atom. The principle importance of these  ${}^1E-{}^3A_1$  intersystem crossings is not only connected with wavelength selectivity of the Mn–H and Co–H photodissociation<sup>92,93</sup>, but also with the fact that the  $S \rightarrow T$  transition at the intermediate stage of dissociation provides stability of the produced active catalyst intermediate – triplet radical pair. For example, if the produced radical pair  $H + Mn(CO)_5$  would be formed in the singlet state, it must recombine immediately. The dissociation through the triplet state prevents the reverse recombination and provides the catalyst  $Mn(CO)_5$  from going out into the bulk. Quite similar ideas could be applied to photochemistry of rhenium complexes<sup>95</sup>  $(\eta^1-R)Re(CO)_5$ . Near-UV irradiation yields predominantly radical products, whereas thermolysis yields only CO loss. The photochemical Re–R bond cleavage giving  $Re(CO)_5$  and R radicals does not finish by the mutual recombination in geminate pairs; the ultimate radical products are<sup>95</sup>  $Re_2(CO)_{10}$  and  $R_2$ . It could be possible only if the S–T nonradiative transitions occur during photodissociation.

## 5. PARAMAGNETIC EXCHANGE SPIN-CATALYSIS

Catalysis of some homogeneous chemical reactions by paramagnetic substances has been known for over half a century<sup>7,96,97</sup>. For example, the rare-earth ions accelerate the rate of decarboxylation of malonic acid derivatives<sup>7</sup>. Another example of particular relevance is the catalysis of *cis-trans* isomerization of olefins by paramagnetic gases<sup>97</sup>. All these processes constitute examples of homogeneous spin-catalysis of the second type. This type of catalysis is denoted as “paramagnetic” because it is produced by paramagnetic species, but it has no relation to the magnetic field perturbations produced by catalysts<sup>4,5,98</sup>. The nature of this catalysis is determined by intermolecular exchange interactions (electronic correlation effects) and by charge-transfer interactions<sup>4</sup>.

The simplest example of this type of spin-catalysis is represented by the  $[{}^2H_2]$ -ethylene gas phase thermal *cis-trans* isomerization reaction, catalyzed by  $O_2$ . Eyring et al.<sup>96,99</sup> have interpreted this isomerization reaction on the basis of absolute rate theory, in terms of their well-known “singlet” and “triplet” mechanisms according to whether the reaction proceeds entirely via the singlet state PES or involves a switch to the triplet state (at the torsion angle less than  $90^\circ$ ). The isomerization should proceed by the singlet mechanism in the absence of  $O_2$  collisional perturbations, since the SOC connecting the S and T states should be very small<sup>96</sup>. *Ab initio* calculations of SOC effects in twisted and pyramidalized ethylene<sup>100,101</sup> support this supposition.

Eyring and Harman proposed<sup>99</sup> that paramagnetic substances would catalyze the triplet mechanism by providing a non-homogeneous magnetic field which will act differently on each of the two magnetic dipoles arising from the spin of the two electrons of

the double bond. Estimations show, however, that this effect is negligible<sup>37</sup>. An alternative explanation of catalytic action has been put forward by McConnell<sup>102</sup>. He suggested that the catalyst in an electronic state other than the singlet state interacts with the S and T states of the isomer and that the resulting electronic states are such as to allow an alternative nonadiabatic reaction path.

In the collision complex between O<sub>2</sub> and ethylene both the singlet ground and triplet excited states of the ethylene moiety have triplet character because of the two unpaired electrons of the oxygen. The thermally induced S–T transition during the CH<sub>2</sub> group rotation in such a catalytic system is not spin-forbidden and its probability depends on the configuration interaction (CI) in the collision complex<sup>4,103</sup>. The CI includes intermolecular exchange and charge transfer interactions, the latter being quite important<sup>4</sup>. If this intermolecular CI is large we can speak about the “S–T” avoided crossing in the organic substrate. This mechanism is similar to the mechanism of the S–T transition enhancements in unsaturated hydrocarbons induced by paramagnetic species<sup>4,103</sup>. Such enhancements have been observed in absorption and in nonradiative processes induced by molecular oxygen<sup>22,104</sup>. Comparison with the EHA induced S–T absorption indicates the similarity of the spectra<sup>22</sup>, but the nature of these physical spin-catalytic perturbations is completely different<sup>38,40,103,105</sup>; for the EHA effect the SOC is responsible for removing of spin prohibition while for the oxygen induced S–T transition enhancement the exchange and charge transfer interactions<sup>37</sup> are responsible, without involving magnetic perturbations. The direct CI calculations<sup>103,105</sup> have supported these ideas.

The rotation around the C=C bond actually increases the charge transfer admixtures in activated complexes formed with paramagnetic O<sub>2</sub> catalysts; the probability of the “S–T” transition inside the ethylene moiety determined by the avoided crossing of two triplet potential energy surfaces is also increased by these admixtures. By the MNDO CI method we have found a small decrease of activation energy (1 – 2 kcal/mol) for the CH<sub>2</sub> group rotation in ethylene being in complex with O<sub>2</sub> at large intermolecular distances (3.8 – 3.4 Å). The results are shown in Fig. 9 for the shortest O–C distance of 3.4 Å. The geometry of collision is similar to that shown on Fig. 7 for the diradical formation reaction. *Ab initio* CI calculations in STO-6G basis set for the same collision complex have been performed scanning the rotational angle in ethylene. The barrier for rotation around the C–C bond in the singlet ground state has been obtained equal to 64.87 kcal/mol in pure ethylene. The plane and 90°-twisted singlet ethylene energies are –77.873 and –77.770 a.u. respectively for partial geometry optimization, i.e. C–C bond prolongation (the triplet twisted ethylene has an energy of –77.770 a.u., so it is only 0.54 kcal/mol more stable than the singlet one). In contact with oxygen at R(C–O) = 2.4 Å the corresponding “singlet” state energies become equal to –266.958 and –226.857 a.u., respectively, so the activation barrier for the “singlet” state isomerization is 62.89 kcal/mol (this is the triplet state in the collision complex with O<sub>2</sub>.) The energy of O<sub>2</sub>(<sup>3</sup>Σ<sub>g</sub><sup>-</sup>) is –149.099 a.u. at the same level. The singlet, triplet and quintet states corresponding to

the T-T pair have energies  $-226.862313$ ,  $-226.862127$  and  $-226.858057$  a.u., respectively. It means that the "avoided S-T crossing" on the ground (triplet) potential energy surface because of the contact with paramagnetic catalyst produces the further decrease of activation barrier for isomerization reaction (59.92 kcal/mol). The total lowering of activation energy approximately by 5 kcal/mol in such spin-catalysis has been obtained<sup>106</sup>. This configuration interaction referring to the intermolecular exchange mixing and repulsion of local S and T states determines the nature of the paramagnetic spin-catalysis.

## 6. OXYGEN ACTIVATION BY METAL COMPLEXES AND OXIDATION SPIN-CATALYSTS

As it was mentioned before, important examples of spin-catalysis are given by O<sub>2</sub> reactivity. The ground triplet state,  $^3\Sigma_g^-$ , of molecular oxygen cannot react directly with

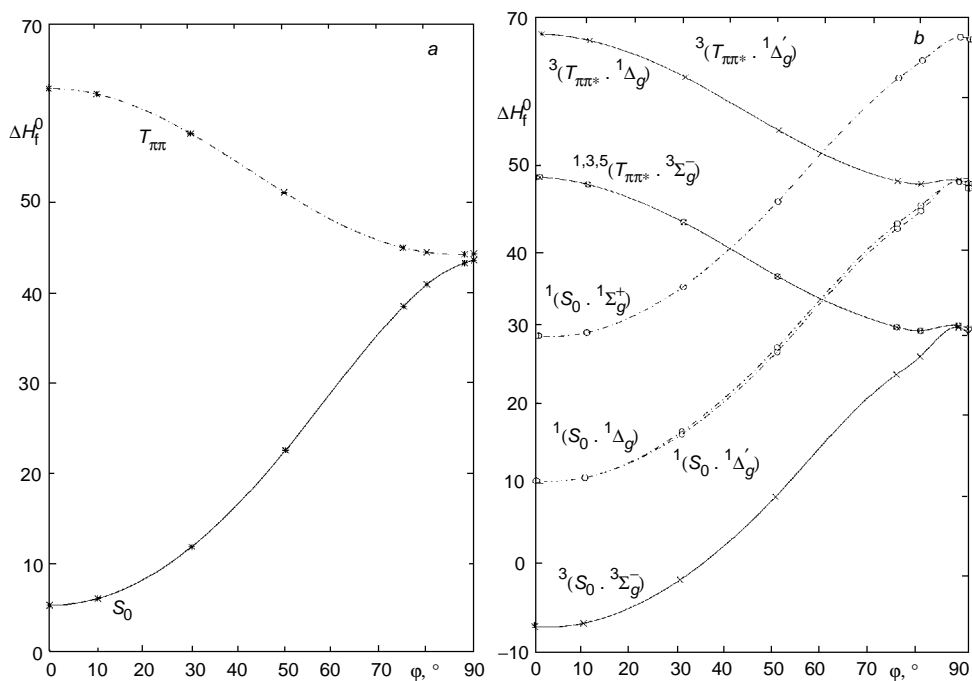


FIG. 9

Cross sections of potential energy surface along the reaction path for the HCH-group rotation around the C-C bond of ethylene: *a* free ethylene, *b* ethylene in contact with the molecular oxygen (distance between oxygen and carbon atoms is equal to 3.4 Å). Abscissa axis denotes heats of formation in kcal/mol. Ordinate axis denotes rotational angle in degrees

diamagnetic substances to produce chemically stable diamagnetic products of oxidation because of spin-prohibition. This is a reason for that a large variety of such processes proceed through radical chain reactions<sup>4,107</sup>. The second general kinetic restriction on the reactions of O<sub>2</sub> is that in a stepwise one-electron reduction mechanism the addition of electrons into molecular oxygen is thermodynamically unfavorable<sup>108</sup> (O<sub>2</sub> + e<sup>-</sup> → O<sub>2</sub><sup>-</sup>, E<sup>0</sup> = -0.33 V for O<sub>2</sub> at 10<sup>6</sup> Pa. The kinetically controlled sluggish reactivity of molecular oxygen from air thus allows for control and tuning by spin-catalysis. The reactions of <sup>3</sup>O<sub>2</sub> with compounds which are diamagnetic having redox potentials forbidding an outer-sphere electron transfer must find a way to circumvent the spin barrier<sup>4,109</sup>. The theoretical treatments explaining that some O<sub>2</sub>-substrate couples undergo such thermally induced intersystem crossings are presented in refs<sup>4,5,74,107,109</sup> including all types of spin-catalysis. The comprehensive understanding of these mechanisms could be of importance for the manufacturing of catalysts that will provide effective oxidizing synthesis.

There are two means by which O<sub>2</sub> is activated in biological systems. The first constitutes reactions that become spin-allowed by substrate activation. These are the reactions of triplet O<sub>2</sub> with radical substrates and with substrates to form products with low-lying triplet states. The former could be produced by outer-sphere redox processes for favorable catalyst-organic substrate pairs. The latter occur with flavin enzymes, for example, when O<sub>2</sub> reacts with a reduced flavin to form a low energy triplet complex which can decay to a singlet state product<sup>108</sup>.

The most common pathway for oxygen activation is via the mediation of a metal ion catalyst<sup>76,108</sup>. The large SOC in metal ions and the inclusion of its *d* orbitals reduces the kinetic barrier for the spin change. Also, bonding of the metal to O<sub>2</sub> itself may provide sufficient energy to overcome spin-pairing energy barriers and to remove both the spin and the thermodynamic restrictions<sup>108,110</sup>. It was shown<sup>55</sup> that charge transfer interactions with donor molecules directly increase SOC between the ground triplet and the *a*<sup>1</sup>Δ<sub>g</sub> states of O<sub>2</sub>, which help to overcome spin prohibition. So the redox properties of catalysts and reactants are connected with spin-catalysis of oxidation by molecular oxygen<sup>5</sup>. Although the strict definition of metal activation of O<sub>2</sub> is not always clear<sup>108</sup>, we can suspect that both the two main types of thermal spin-catalysis can operate here.

## 7. SUMMARY

The examples presented in this work show the importance of spin-orbit coupling effects in organic chemical reactions and of spin-crossover phenomena in transition metal compounds. These examples, together with magnetic field effects in chemical reactivity, give the general links between catalytic action and different types of spin uncoupling. This work presents the first attempt to specify and classify spin-catalysis phenomena. These phenomena appear to be quite general and are especially important for biochemistry.

A number of known phenomena fall into the definition of spin-catalysis given in this article. They can be classified according to two main categories: (i) spin-orbit coupling induced – and, (ii) paramagnetic-exchange induced spin-catalysis. Other types of spin-catalysis are also shortly discussed. These are (iii) the numerous photosensitized reactions proceeding by triplet-triplet energy transfer or by singlet  $^1\Delta$  oxygen generation. Spin-prohibition in these cases is overcome during the singlet-triplet intersystem crossing inside the sensitizer (spin-catalyst) and then transferred by a spin-conserving energy transfer processes to the catalyzed reacting system. (iv) Substances which assist in thermal or electrochemical generation of active particles (radicals, diradicals,  $O_2(^1\Delta_g)$  etc.), reacting further without spin-prohibition. (v) The process induced by an external magnetic field and magnetic isotope spin-catalysis.

The processes (iii), (iv) and (v) are quite general and well-known; their inclusion in the spin-catalysis classification unite them with the important catalytic processes of the first two types. This seems to be a useful guide in catalysis theory and in chemical kinetics. Combination and interconnections of different types of these catalytic processes are possible and are often quite important. They are known in biosystems and particularly in photosynthesis.

The spin-catalysis concept stresses the importance of factors which depend on spin states of both moieties, catalyst and catalysant, in the activated complex. The processes of the second type do not include any total spin change of the catalytic system, although the spin coupling inside each moiety is changed. Therefore they relate to many other catalytic processes with diamagnetic ground state reagents, which include spin-uncoupling in the transition region. The configuration interaction admixture of two triplet excited state configurations from the two molecules to the singlet ground state PES is a typical example for many chemical reactions and catalytic processes. So the spin-catalysis concept helps to understand the nature of catalytic actions in general. A few models of spin-catalytic processes and SOC induced reactions have been simulated for the purpose of illuminating the principles of spin-catalysis.

## ACRONYMS

CIDNP	chemically induced dynamic nuclear polarization
CT	charge transfer
EHA	external heavy atom
ISC	intersystem crossing
MF	magnetic field
PES	potential energy surface
RP	radical pair
RPT	radical pair theory
SLR	spin-lattice relaxation
SOC	spin-orbital coupling
ZFS	zero field splitting

*This work was supported by grants from the Royal Swedish Academy of Science (BFM) and from CRAY Research Inc. (HÅ). The assistance of O. Plashkevich in calculations is gratefully acknowledged.*

## REFERENCES

1. Salem L.: *Electrons in Chemical Reactions: First Principles*. Wiley, New York 1982.
2. Minaev B. F.: *Dr. Sc. Thesis*. Chem. Phys. Institute, Moscow 1983.
3. Minaev B. F., Lunell S.: *Z. Phys. Chem.* **182**, 263 (1993).
4. Minaev B. F.: *Zh. Strukt. Khim.* **23**, 7 (1982).
5. Minaev B. F., Dausheev Z. K. in: *The 8th USSR Conference on Heterogeneous Catalysis. Spin-Catalysis in Hydrocarbon Oxidation Process*, p. 209. Institute of Electrochemistry and Catalysis, Alma Ata 1988.
6. Fisher M., Sligar S. G.: *Biochemistry* **26**, 4797 (1987).
7. Pitzer K. S., Geller E.: *J. Am. Chem. Soc.* **75**, 5132 (1953).
8. Douglas J. E., Rabinovitch B. S., Looney F. S.: *J. Chem. Phys.* **23**, 315 (1955).
9. Tchougreeff A. L., Misurkin I. A.: *Chem. Phys.* **133**, 77 (1989).
10. Anders J., Safont V. S., Tapia O.: *Chem. Phys. Lett.* **198**, 515 (1992).
11. Clark T.: *J. Am. Chem. Soc.* **111**, 761 (1989).
12. Mango F. D., Schachtschneider J. H.: *J. Am. Chem. Soc.* **93**, 1123 (1971).
13. Kearns D. R.: *Chem. Rev.* **71**, 395 (1971).
14. Muldahmetov Z. M., Minaev B. F., Zhurinov M. Z.: *Quantum Electrochemistry of Alkaloids*. (Russ.) Nauka, Alma Ata 1985.
15. Steiner U. E., Ulrich T.: *Chem. Rev.* **89**, 51 (1989).
16. Salikhov K. M., Molin Yu. N., Sagdeev R. Z., Buchachenko A. L.: *Magnetic and Spin Effects in Chemical Reactions*. Elsevier, Amsterdam 1984.
17. Muldahmetov Z. M., Minaev B. F., Ketsle G. A.: *Optical and Magnetic Properties of the Triplet State*. Nauka, Alma Ata 1983.
18. Doubleday C., Turro N. J., Wang J.-F.: *Acc. Chem. Res.* **22**, 199 (1989).
19. Minaev B. F.: *Opt. Spektrosk.* **21**, 11 (1972).
20. Minaev B. F.: *PhD Thesis*. Tomsk State University, Tomsk 1973.
21. Minaev B. F.: *Fizika Molekul*. Naukova Dumka, Kiev 1979.
22. McGlynn S. P., Azumi T., Kinoshita M.: *Molecular Spectroscopy of the Triplet State*. Prentice Hall, Englewood Cliffs, NJ 1969.
23. Minaev B. F., Kizner D. M.: *Collect. Czech. Chem. Commun.* **46**, 1318 (1981).
24. Turro N. J.: *Pure Appl. Chem.* **27**, 679 (1971).
25. Salem L.: *J. Am. Chem. Soc.* **96**, 3486 (1974).
26. Freilich S. C., Peters K. S.: *J. Am. Chem. Soc.* **103**, 6255 (1981).
27. Palmer I. J., Ragazos I. N., Bernardi F., Olivucci M., Robb M. A.: *J. Am. Chem. Soc.* **116**, 2121 (1994).
28. Freilich S. C., Peters K. S.: *J. Am. Chem. Soc.* **107**, 3819 (1985).
29. Minaev B. F.: Unpublished results.
30. Turro N., Devaquet A.: *J. Am. Chem. Soc.* **97**, 3859 (1975).
31. Dewar M. J. S., Kirschner S.: *J. Am. Chem. Soc.* **96**, 7578 (1974).
32. Srinivasan R.: *Pure Appl. Chem.* **16**, 65 (1968).
33. Muldahmetov Z. M., Minaev B. F., Ketsle G. A.: *The External Heavy Atom Effects in Photochemistry and Photophysics*. Nauka, Alma Ata 1987.
34. Kasha M.: *J. Chem. Phys.* **20**, 71 (1952).

35. Amirav A., Even U., Jortner J.: Chem. Phys. Lett. 67, 9 (1979).
36. Hoihtink G. J.: Mol. Phys. 3, 67 (1960).
37. Tsubamura H., Mulliken R. S.: J. Am. Chem. Soc. 82, 5666 (1960).
38. Minaev B. F., Knuts S., Agren H.: Chem. Phys. 181, 15 (1994).
39. Vahtras O., Agren H., Jorgensen P., Jensen H. J. Aa., Helgaker T., Olsen J.: J. Chem. Phys. 96, 2118 (1992).
40. Minaev B. F.: Zh. Prikl. Khim. 43, 131 (1985).
41. Inoue H., Sakurai T., Hoshi T.: J. Photochem. Photobiol., A 72, 41 (1993).
42. Cooper W., Rome K. A.: J. Phys. Chem. 78, 16 (1974).
43. Sveida P., Maki A. H., Anderson R. R.: J. Am. Chem. Soc. 100, 7138 (1978).
44. Rahn R. O., Laundry L. C.: Photochem. Photobiol. 18, 29 (1973).
45. Sauerwein B., Schuster G. B.: J. Phys. Chem. 95, 1903 (1991).
46. Steiner U. E., Haas W.: J. Phys. Chem. 95, 1880 (1991).
47. Levin P. P., Kuzmin V. A.: Chem. Phys. Lett. 165, 302 (1990).
48. Kikuchi K., Hoshi M., Niwa T., Takahashi Y., Miyashi T.: J. Phys. Chem. 95, 38 (1991).
49. Minaev B. F., Terpugova A. F.: Izv. Vyssh. Ucheb. Zaved., Fiz. 10, 30 (1969).
50. Minaev B. F., Terpyuyova A. F. in: *Theory of Electronic Shells in Atoms and Molecules* (A. P. Jucis, Ed.), p. 321. Mintis, Vilnius 1971.
51. Minaev B. F.: Izv. Vyssh. Ucheb. Zaved., Fiz. 5, 160 (1978).
52. Minaev B. F.: Opt. Spektrosk. 44, 148 (1978).
53. Minaev B. F., Serebrennikov Yu. A.: Izv. Vyssh. Ucheb. Zaved., Fiz. 5, 27, 1978.
54. Ketsle G. A., Levshin L. V., Melnikov G. A., Minaev B. F.: Opt. Spektrosk. 51, 655 (1981).
55. Minaev B. F.: Teor. Eksp. Khim. 20, 209 (1984).
56. Minaev B. F., Irgibaeva I. S., Muldahmetov Z. M.: Teor. Eksp. Khim. 20, 305 (1984).
57. Minaev B. F., Irgibaeva I. S., Muldahmetov Z. M.: Izv. Akad. Nauk. KazSSR, Ser. Khim. 6, 61 (1984).
58. Serebrennikov Yu. A., Minaev B. F., Abdrahmanov B. M.: Khim. Fiz. 5, 878 (1986).
59. Serebrennikov Yu. A., Minaev B. F.: Chem. Phys. 114, 359 (1987).
60. Bohling R., Becker A., Serawski K., Minaev B. F., Schurath U.: Chem. Phys. 142, 445 (1990).
61. Minaev B. F., Danilovich I. M., Serebrennikov Yu. A. in: *Dynamics of Triplet Excitations in Molecular Crystals* (M. A. Shpak, Ed.), p. 109. Naukova Dumka, Kiev 1989.
62. Ketsle H. A., Kucherenko M. G., Minaev B. F. in: *Dynamics of Triplet Excitations in Molecular Crystals* (M. A. Shpak, Ed.), p. 100. Naukova Dumka, Kiev 1989.
63. Minaev B. F., Bryukhanov V. V., Laurinas V. D.: Zh. Prikl. Spektrosk. 50, 216 (1985).
64. Bryukhanov V. V., Minaev B. F., Kusenova A. S., Karstina S. G.: Zh. Prikl. Spektrosk. 56, 229 (1992).
65. Minaev B. F., Lunell S., Kobzev G. I.: Theochem., J. Mol. Struct. 284, 1 (1993).
66. Minaev B. F., Irgibaeva I. S., Muldahmetov Z. M.: Teor. Eksp. Khim. 17, 659 (1981).
67. Bryukhanov V. V., Ketsle G. A., Levshin L. V., Minaev B. F.: Opt. Spectrosk. 45, 868 (1978).
68. Melnikov G. V., Ketsle G. A., Minaev B. F. in: *The Nuclear and Electron Spin Polarization and Magnetic Field Effects in Chemical Reactions* (I. P. Gragerov, Ed.), p. 55. L. V. Pisarzhevsky Institute of Physical Chemistry, Kiev 1978.
69. Serebrennikov Yu. A., Minaev B. F., Mukhin R. R.: Zh. Fiz. Khim. 63, 730 (1989).
70. Atkins P. W., Evance G. T.: Mol. Phys. 27, 1633 (1974).
71. Toftlund H.: Coord. Chem. Rev. 94, 67 (1989).
72. Bacci M.: Coord. Chem. Rev. 86, 245 (1988).
73. Perito R. P., Corden B. B.: J. Am. Chem. Soc. 109, 4418 (1987).
74. Minaev B. F.: Zh. Fiz. Khim. 66, 2992 (1992).



75. Coryell C. D., Stitt F., Pauling L., *J. Am. Chem. Soc.* *59*, 633 (1937).
76. Gubelmann M. H., Williams A. F.: *Structure and Bonding*, Vol. 55, p. 1. Springer, Berlin (1983).
77. Tamura M.: *Biochim. Biophys. Acta* *243*, 239 (1971).
78. Armentrout P. B.: *Ann. Rev. Phys. Chem.* *41*, 313 (1990).
79. Sheldon R. A., Kochi J. K.: *Metal-Catalyzed Oxidation of Organic Compounds*. Academic Press, New York 1981.
80. Mitchell S. A., Blitz M. A., Siegbahn P. E. M., Svensson M.: *J. Chem. Phys.* *100*, 423 (1994).
81. Clemmer D. E., Chen Y. M., Khan F. A., Armentrout P. B.: *J. Phys. Chem.* *98*, 6522 (1994).
82. Fox M. A., Dulay M. T.: *Chem. Rev.* *93*, 341 (1993).
83. Fujishima A., Honda K.: *Nature* *37*, 238 (1972).
84. Minaev B. F., Serevrennikov Yu. A., Rempel G.: *Phys. Status Solidi. B* *142*, 689 (1988).
85. Kiwi J.: *J. Phys. Chem.* *87*, 2274 (1983).
86. Steiner U. E., Haas W., Wolff H. J., Burschner D.: *Proc. Indian Acad. Sci., Chem. Sci.* *104*, 229 (1992).
87. Schwab G., Kaiser A.: *Z. Phys. Chem.* *22*, 220 (1959).
88. Buchachenko A. L.: *Zh. Fiz. Khim.* *51*, 1445 (1977).
89. Samarskaya T. G., Skrunts L. K., Kiprianova L. A., Levit I. P., Gragerov I. P.: *Dokl. Akad. Nauk SSSR, Phys. Chem.* *283*, 697 (1985).
90. Geoffroy G. L.: *Prog. Inorg. Chem.* *27*, 123 (1980).
91. Mrgehee E. G., Meyer T. J.: *Inorg. Chem.* *28*, 4084 (1989).
92. Veillard A.: *Chem. Phys. Lett.* *170*, 441 (1990).
93. Daniel C.: *J. Am. Chem. Soc.* *114*, 1625 (1992).
94. Minaev B. F., Agren H.: *Int. J. Quantum Chem.*, in press.
95. Young K. M., Miller T. M., Wrighton M. S.: *J. Am. Chem. Soc.* *112*, 1529 (1990).
96. Magee J. L., Shand W., Eyring H.: *J. Am. Chem. Soc.* *63*, 677 (1941).
97. Tamamushi B., Akijama H.: *Bull. Chem. Soc. Jpn.* *12*, 382 (1937).
98. McClure D. S.: *J. Chem. Phys.* *20*, 682 (1952).
99. Harman R. A., Eyring H.: *J. Chem. Phys.* *10*, 557 (1942).
100. Caldwell R. A., Carlucci L., Doubleday C. E., Furlani T. R., King H. F., McIver J. W., jr.: *J. Am. Chem. Soc.* *110*, 6901 (1988).
101. Minaev B. F., Norman P., Jonsson D., Ågren H.: *Chem. Phys.*, in press.
102. McConnell H.: *J. Chem. Phys.* *20*, 1043 (1952).
103. Minaev B. F., Kukueva V. V., Agren H.: *J. Chem. Soc., Faraday Trans.* *90*, 1479 (1994).
104. Evans D. F.: *J. Chem. Soc.* *1960*, 1735.
105. Minaev B. F.: *Zh. Prikl. Spektrosk.* *42*, 766 (1985).
106. Minaev B. F., Plashkevich O. N., Ågren H.: *Zh. Fiz. Khim.*, in press.
107. Minaev B. F.: *Khim. Fiz.* *3*, 983 (1984).
108. Karlin K. D., Gulten Y.: *Prog. Inorg. Chem.* *35*, 219 (1987).
109. Minaev B. F., Thihomirov V. A., Daushev Z. K.: *Khim. Fiz.* *3*, 615 (1984).
110. Herman Z. S., Loew G. H.: *J. Am. Chem. Soc.* *102*, 1815 (1980).